© 2020. Published by The Company of Biologists Ltd | Biology Open (2020) 9, bio055343. doi:10.1242/bio.055343

METHODS & TECHNIQUES

Stable integration of an optimized inducible promoter system enables spatiotemporal control of gene expression throughout avian development

Daniel Chu, An Nguyen*, Spenser S. Smith*, Zuzana Vavrušová* and Richard A. Schneider‡

ABSTRACT

Precisely altering gene expression is critical for understanding molecular processes of embryogenesis. Although some tools exist for transgene misexpression in developing chick embryos, we have refined and advanced them by simplifying and optimizing constructs for spatiotemporal control. To maintain expression over the entire course of embryonic development we use an enhanced *piggyBac* transposon system that efficiently integrates sequences into the host genome. We also incorporate a DNA targeting sequence to direct plasmid translocation into the nucleus and a D4Z4 insulator sequence to prevent epigenetic silencing. We designed these constructs to minimize their size and maximize cellular uptake, and to simplify usage by placing all of the integrating sequences on a single plasmid. Following electroporation of stage HH8.5 embryos, our tetracycline-inducible promoter construct produces robust transgene expression in the presence of doxycycline at any point during embryonic development *in ovo* or in culture. Moreover, expression levels can be modulated by titrating doxycycline concentrations and spatial control can be achieved using beads or gels. Thus, we have generated a novel, sensitive, tunable, and stable inducible-promoter system for high-resolution gene manipulation *in vivo*.

KEY WORDS: Gene expression, *PiggyBac* transposon, Tet-inducible, Avian embryos

INTRODUCTION

For thousands of years, birds have been used to study development. The ability to 'window' and reseal the egg shell, the comparatively large size of the embryo, the straightforward process of stage-matching diverse embryos, the ease of starting and arresting embryogenesis at any time, and the commercial availability of fertilized eggs have significantly advanced the utilization of birds for a broad range of experiments (Stern, 2005; Jheon and Schneider, 2009). Birds remain particularly applicable for questions that are best answered through microsurgical manipulations (e.g. tissue recombination, transplants, ablation, or extirpations), cell labeling and live imaging (e.g. fluorescent dyes and other agents, *ex ovo* culture, or immunochemical detection of engrafted cells), gain- and loss-of-function strategies (e.g. implantation of reagent-soaked beads, insertion of cell pellets, injection of biochemicals, infection with retroviruses, or electroporation of constructs) and other experimental approaches (Johnston, 1966; Noden, 1975; Serbedzija et al., 1989; Fekete and Cepko, 1993b; Stocker et al., 1993; Bronner-Fraser, 1996; Chen et al., 1999; Kulesa and Fraser, 2000; Larsen et al., 2001; Nakamura and Funahashi, 2001; Schneider et al., 2001; Garcia-Castro et al., 2002; Trainor et al., 2002; Cerny et al., 2004; Krull, 2004; Lwigale et al., 2004; Lwigale et al., 2005; Schneider, 2007; Bronner-Fraser and Garcia-Castro, 2008; Lwigale and Schneider, 2008; Sauka-Spengler and Barembaum, 2008; Fish and Schneider, 2014; Fish et al., 2014; Ealba et al., 2015; Woronowicz et al., 2018). Overall, such strategies have been indispensable to understanding numerous dynamic aspects of development including cell fate decisions, tissue interactions, pattern formation, morphogenesis, and gene function and regulatory networks (Le Douarin and McLaren, 1984; Noden, 1984; Le Douarin et al., 1996; Clarke and Tickle, 1999; Schneider, 1999; Eames and Schneider, 2005; Noden and Schneider, 2006; Sauka-Spengler and Bronner-Fraser, 2008; Tokita and Schneider, 2009; Betancur et al., 2010; Le Douarin and Dieterlen-Lièvre, 2013; Martik and Bronner, 2017; Abramyan and Richman, 2018; Schneider, 2018; Gammill et al., 2019; Núñez-León et al., 2019).

However, there are limitations to what can be done with avian embryos. For example, compared to mouse or zebrafish model systems, birds have limited genetic tools, transgenic lines are expensive to maintain, and targeted mutagenesis followed by forward genetics is difficult. While some transgenic chick and quail lines have been generated (McGrew et al., 2004; Chapman et al., 2005; Koo et al., 2006; van de Lavoir et al., 2006a,b; Sato et al., 2010; Bower et al., 2011; Huss et al., 2015; June Byun et al., 2017; Tsujino et al., 2019), the technical challenges and expense of making transgenics, the low efficiency of transgene inheritance due to epigenetic silencing or selection against transgenic germ cells/gametes, combined with the logistics of keeping sufficient transgenic flocks has limited the broad application of this approach (Sang, 2006; Park et al., 2010; Macdonald et al., 2012; Liu et al., 2013; Bednarczyk et al., 2018). Nonetheless, the ability to create genetic mutations through CRISPR/Cas9 technology has already made the prospects of genome engineering much easier in avians (Ahn et al., 2017; Gandhi et al., 2017; Morin et al., 2017; Williams et al., 2018).

Given the challenges of germ line transgenesis, proxies for studying gene function in avian model systems have predominantly involved a range of alternative strategies. For example, transgenes can be delivered efficiently using retroviral vectors (Fekete and Cepko, 1993a; Morgan and Fekete, 1996; Logan and Tabin, 1998; Chen et al., 1999; Kardon et al., 2003; Hughes, 2004) especially the

Department of Orthopaedic Surgery, University of California at San Francisco, 513 Parnassus Avenue, S-1164, San Francisco, CA 94143-0514, USA.

*These authors contributed equally and are listed alphabetically

‡Author for correspondence (rich.schneider@ucsf.edu)

R.A.S., 0000-0002-2626-3111

Received 24 July 2020; Accepted 27 August 2020

Biology Open

Biology Open (2020) 9, bio055343. doi:10.1242/bio.055343

replication-competent RCAS and RCASBP retroviruses. Some advantages of these vectors include their ability to spread widely throughout host tissues, which in turn allows for broad misexpression of a given transgene, and the ease at preparing large quantities of high-titer viral stocks (Logan and Tabin, 1998). But some limitations of retroviral vectors include the size of the gene insert that they can carry (up to approximately 2.4 kb), as well as their inability to infect most strains of chickens and other birds because of immunity arising from prior exposure to avian sarcoma-leukosis viruses (Hughes, 2004). A further drawback of retroviral-based strategies is their general lack of precise control over the timing, spatial domains, and levels of gene misexpression. Oftentimes, to achieve sufficient amounts of viral spread, infection must be performed at very early stages, which means that the transgene has to be expressed continuously throughout development regardless if there is a specific stage desired for expressing genes of interest.

Another approach for transiently misexpressing genes in a given location or for a certain period of time relies on electroporation of promoter-driven DNA constructs. Electroporation, which is very effective in avian embryos, involves placing electrodes to generate a pulsed electric field that transiently alters the plasma membrane and allows DNA constructs to be introduced into cells (Funahashi et al., 1999; Itasaki et al., 1999; Momose et al., 1999; Nakamura and Funahashi, 2001; Swartz et al., 2001; Chen et al., 2004; Krull, 2004; Simkin et al., 2014; Reberšek, 2017; McLennan and Kulesa, 2019). Electroporation is a very effective technique for introducing expression constructs into the premigratory cephalic NCM particularly by targeting the neural folds in stage HH8.5 embryos (Creuzet et al., 2002; Krull, 2004; McLennan and Kulesa, 2007; Hall et al., 2014). Several DNA constructs containing a robust chicken β-actin promoter, a CMV promoter, an internal ribosome entry site (IRES), and a bicistronic reporter with green fluorescent protein (GFP) have been widely adopted including pMES, pCIG, and pCAβ (Swartz et al., 2001; Megason and McMahon, 2002; McLarren et al., 2003; Sauka-Spengler and Barembaum, 2008; Jhingory et al., 2010; Hall et al., 2014; Yang et al., 2014; Gammill et al., 2019; Wu and Taneyhill, 2019). Electroporation can also efficiently enable gene repression using RNA interference (RNAi) and antisense morpholino oligonucleotides (Tucker, 2001; Kos et al., 2003; Chesnutt and Niswander, 2004; Krull, 2004; Nakamura et al., 2004; Rao et al., 2004; Das et al., 2006; Sauka-Spengler and Barembaum, 2008; Gammill et al., 2019). However, due to the extrachromosomal nature of these vectors such treatments are only transient since plasmids and short oligonucleotides degrade and dilute following the proliferation of transfected cells, and misexpression is almost entirely eliminated by 72 to 96 h (Sauka-Spengler and Barembaum, 2008; Wang et al., 2011; Hall et al., 2014; Bourgeois et al., 2015). Moreover, the promoters in these widely used plasmids cannot be induced to control the timing or levels of gene expression. Thus, there has remained a need for highly versatile vectors that can achieve both long-term and conditional expression in avian embryos. To this end, one transgene expression system was created that uses *Tol2* transposon-mediated gene transfer (Koga et al., 1996) to enable stable integration of a given transgene into the avian genome (Kawakami, 2007), and that leverages a tetracycline (tet)-dependent inducible promoter (Sato et al., 2007; Watanabe et al., 2007; Takahashi et al., 2008). This system has been useful, for example, for studying the behavior and activity of neural crest mesenchyme (NCM) during later stages of embryogenesis (Yokota et al., 2011).

Building on the clear advantages of inducible promoter systems for exerting spatiotemporal control over gene expression and the ability of transposable elements to integrate into the avian genome and facilitate long-term expression throughout development (Wang et al., 2011; Macdonald et al., 2012; Serralbo et al., 2013; Bourgeois et al., 2015), we endeavored to design a new gene delivery system that advances this technology. Our goal was to streamline and minimize the number of components, to optimize the delivery and detection features, and to achieve efficient and more robust transgene expression. To do so, we generated a constitutively active mNeonGreen (GFP) (Shaner et al., 2013) and doxycycline (dox)-inducible (Gossen et al., 1995; Loew et al., 2010; Heinz et al., 2011) mScarlet-I (RFP) (Bindels et al., 2017) construct. Then, to maintain expression of our electroporated constructs throughout embryonic development, we combined our dox-inducible system with an enhanced *piggyBac* transposon system, which allows for stable semi-random integration so that the construct is replicated along with the host genome (Lacoste et al., 2009; Lu et al., 2009; Yusa et al., 2011; Liu et al., 2013; Jordan et al., 2014; Yusa, 2015). We further improved this construct by adding a D4Z4 genetic insulator sequence to block transcriptional repression (Bire et al., 2013) and a DNA targeting sequence (DTS) to direct transport of the plasmids into the nucleus (Dean et al., 1999; Bai et al., 2017). We find that this construct is sensitive to induction by dox both *in ovo* and in culture, integrates stably into the genome of chick and duck, and enables expression in embryonic tissues at any desired time or place. Here we demonstrate for example, that presumptive NCM can be electroporated at embryonic stage (HH) 8.5 and then gene expression can be induced at HH15, HH30, or later. Also, we show that transgene expression levels can be modulated by titrating the concentration of dox, and precise spatial control over transgene activation can be achieved by implanting beads or gels that release dox locally. Thus, our optimized and integrating inducible-promoter system can control the timing, spatial domains, and levels of gene misexpression throughout avian development, which will be useful for a broad range of experimental contexts.

RESULTS AND DISCUSSION

Design of the small plasmid pNano

To maximize transfection and electroporation efficiency we aimed to generate plasmids as small as possible. Smaller plasmids have been shown to transfect and electroporate more efficiently than large plasmids (Yin et al., 2005). Moreover, large plasmids have been found to be toxic when introduced into cells independent of transgene expression from the plasmid (Lesueur et al., 2016). To minimize the size of our constructs we generated a new plasmid, pNano, only including a plasmid origin of replication and β-lactamase resistance (BlaR) sequence with a minimal multicloning site containing EcoRI, EcoRV, and XhoI restriction enzyme sites. The plasmid is 1562 bp (Fig. 1A) and serves as the backbone for the other constructs generated. To our knowledge, pNano is the smallest plasmid with BlaR selection.

Choosing a promoter

We chose the PGK1 promoter over other commonly used promoters due to its relatively small size at 500 bp and its consistent expression across different cell types (Qin et al., 2010; Huss et al., 2015). Moreover, the PGK1 promoter does not contain any viral sequences, which are prone to epigenetic silencing and loss of expression over time (Brooks et al., 2004; Xia et al., 2007; Norrman et al., 2010).

Choosing a transposon

Transient transfections and electroporations with standard plasmids only enable transgene over-expression for up to 5 days, which is

Biology Open (2020) 9, bio055343. doi:10.1242/bio.055343

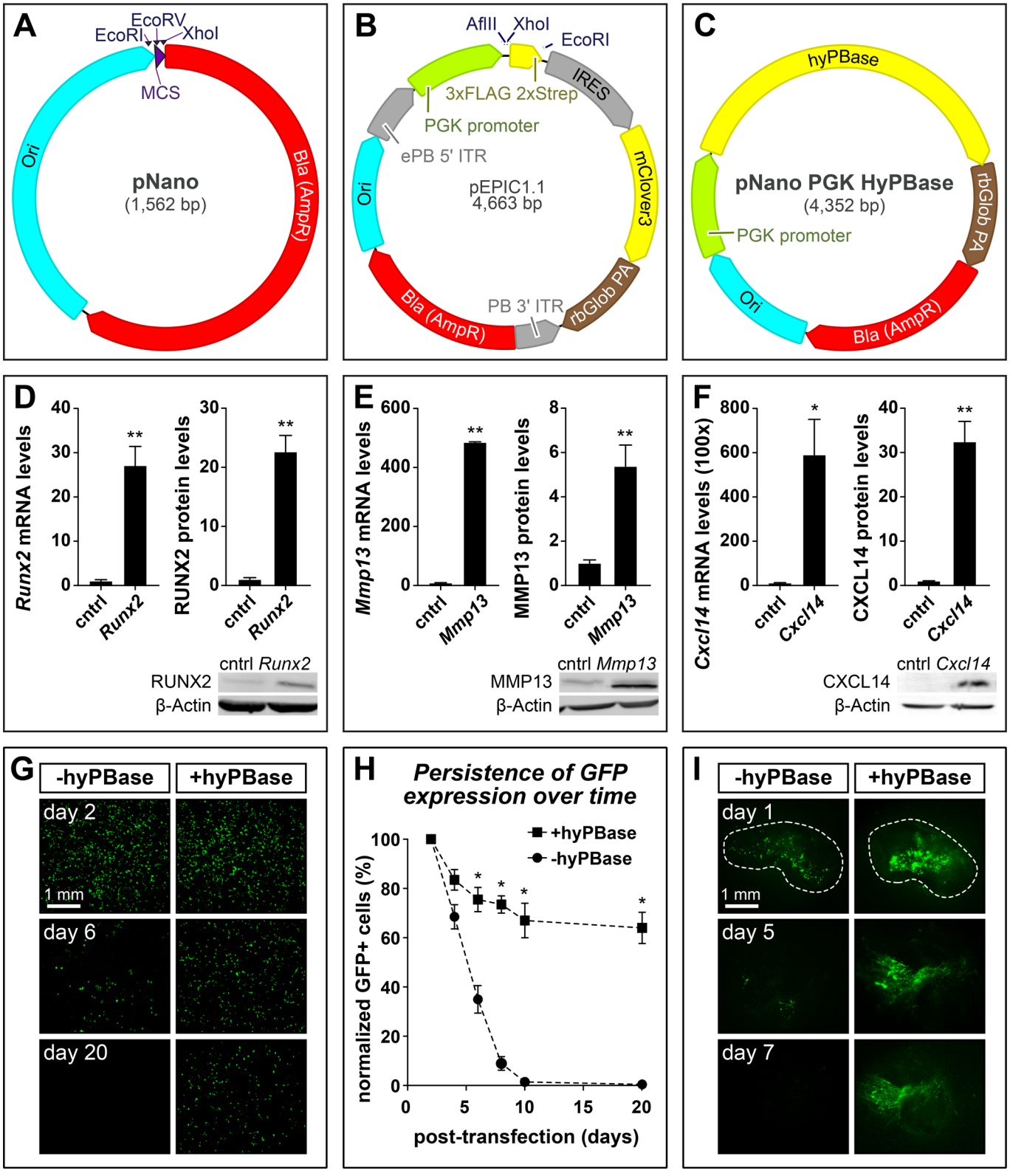

Fig. 1. See next page for legend.

much shorter than the time required to span *in ovo* development (e.g. 21 days for chick and 28 days for duck). To ensure stable and robust expression over the course of embryogenesis, we used a type II transposon (cut and paste) system to integrate sequences into the genome (Curcio and Derbyshire, 2003; Hickman et al., 2010; Yuan and Wessler, 2011). Several transposable systems currently exist including *Tol2* (Koga et al., 1996; Kawakami, 2007), *Sleeping Beauty* (Ivics et al., 1997), and *piggyBac* (Fraser et al., 1983, 1996; Ding et al., 2005). We chose *piggyBac* because previously published work has demonstrated several advantages over other

Biology Open (2020) 9, bio055343. doi:10.1242/bio.055343

Fig. 1. Plasmid maps and over-expression analyses. (A) Map of the pNano minimal cloning vector showing restriction sites for cloning, multicloning sites (MCS) in purple, bacterial origin of replication (Ori) in cyan, and bacterial β-lactamase (Bla) resistance gene (AmpR) in red. (B) Map of the pEPIC1.1 *piggyBac*-integrating constitutively-active expression vector showing *piggyBac* ITRs and IRES sequences in grey, PGK promoter sequences in green, terminator sequences in brown, and coding sequences in yellow. The pEPIC1.1 vector constitutively expresses mClover3, a GFP. (C) Map of the pNano-hyPBase expression vector used to integrate *piggyBac* sequences into host genome. (D) Over-expression of *Runx2*, (E) *Mmp13*, and (F) *Cxcl14* with pEPIC1.1. DF-1 cells were transfected with control (cntrl) empty pEPIC1.1 or pEPIC1.1 plus *Runx2*, *Mmp13*, or *Cxcl14* coding sequences and harvested 3 days post-transfection. Relative mRNA levels were measured by qPCR and normalized using *18S*. Relative protein levels were measured by western blot (WB) and normalized using β-Actin. Representative WBs are shown below. There were four biological replicates for *Runx2* and *Mmp13*, and two for *Cxcl14*. (G) Fluorescent images showing a time course of DF-1 cells transfected with pEPIC1.1. Cells were transfected either without pNano-hyPBase (left column) or with (right column). Cells were passaged every 2 days and imaged at 2, 6, and 20 days post-transfection. (H) Quantification of GFP positive cells as a fraction of the total number of DF-1 cells transfected with pEPIC1.1 with or without pNano-hyPBase and normalized to 2 days post-transfection. There were two biological replicates for each group. (I) Fluorescent images showing a time course of HH21 chick mandibular primordia electroporated with pEPIC1.1-*Cxcl14* either without pNano-hyPBase (left column) or with (right column) cultured, and imaged at day 1, 5, and 7. All qPCR was performed in technical duplicate. A two-tailed *t*-test was used for all statistical analyses. Error bars represent standard error of the mean (s.e.m.). (**P*<0.05; ***P*<0.005).

transposon systems. Most importantly, *piggyBac* shows higher transposition activity than *Tol2* or *Sleeping Beauty* in human and chick (Wu et al., 2006; Lu et al., 2009; Huang et al., 2010) and there are improved versions of both the *piggyBac* transposon and transposase (Lacoste et al., 2009; Yusa et al., 2011). The efficiency of *piggyBac* integration is relatively size independent up to at least 10 kb (Ding et al., 2005) and *piggyBac* can deliver cargos in the hundreds of kb (Li et al., 2011; Rostovskaya et al., 2013), whereas *Sleeping Beauty* has reduced integration efficiency with cargo sizes above 5 kb (Geurts et al., 2003). *PiggyBac* integrates into genomes semi-randomly at sites of open chromatin while *Sleeping Beauty*'s integration pattern appears more random (Huang et al., 2010). In general, successful transposition events into silenced or heterochromatic regions may show no transgene expression due to epigenetic silencing. *PiggyBac* has lower rates of transgene silencing than *Sleeping Beauty* or *Tol2* (Meir and Wu, 2011) and for this reason, the *piggyBac* system can be adapted to enable the expression of transgenes of interest only when they integrate into the genome at a position permissive to transcription (Kumamoto et al., 2020). The *piggyBac* system is also relatively insensitive to the ratio of transposon to transposase while *Sleeping Beauty* and *Tol2* require titration to determine the optimal ratios (Meir et al., 2011). *PiggyBac* has consistent transposition activity across different cell lines (Wu et al., 2006) and has been utilized in many different organisms including yeast, mice, rats, humans, goat, pig, macaque, chick, rice, and several species of protists and insects (Yusa, 2015). This allows for the same construct to be used among different organisms compared to viral methods, which have species-specificity.

Generating the pEPIC1.1 construct for constitutive expression

To enable long-term constitutive transgene expression, we generated pEPIC1.1 (enhanced *piggyBac* IRES mClover3) (Fig. 1B). This construct drives transgene expression under the constitutive PGK promoter. To improve translational efficiency, we included a Kozak sequence directly upstream of the translational start site (Kozak, 1986). As a marker for expression, we used a minimal encephalomyocarditis virus IRES (Bochkov and Palmenberg, 2006) to express a bicistronic transcript containing the over-expressed transgene and mClover3 (GFP) (Bajar et al., 2016). An optional C-terminal tandem affinity purification (TAP) tag consisting of 3xFLAG peptide sequences and 2xStrep-tag II sequences (Dalvai et al., 2015) can be added to enhance detection or pulldown. Sequences can be cloned either untagged by digesting pEPIC1.1 with AflII and EcoRI or tagged by digesting with AflII and XhoI. Sustained expression over long time periods is maintained by flanking the over-expression cassette with *piggyBac* inverted terminal repeat sequences (ITR). The ITRs in the presence of *piggyBac* transposase (PBase) semi-randomly integrates into the host genome at sequences containing a TTAA motif through a cut and paste mechanism. We used the enhanced *piggyBac* sequence which contains two point mutations in the left '5 ITR that increase transposition efficiency (Lacoste et al., 2009). To express PBase we also generated a complementary plasmid, pNano-hyPBase (Fig. 1C). This plasmid expresses a hyperactive version of PBase (hyPBase) (Yusa et al., 2011) under the PGK promoter.

As a proof-of-concept and to test our ability to over-express a diverse range of gene types, we cloned coding sequences of a transcription factor (i.e. *Runx2*, 1419 bp), an extracellular matrix molecule (i.e. *Mmp13*, 1416 bp), and a cytokine (i.e. *Cxcl14*, 297 bp), into pEPIC1.1. We first confirmed that pEPIC1.1 constructs could over-express our genes of interest by transfecting them into a chick fibroblast cell line (DF-1). We found that pEPIC1.1-*Runx2*, pEPIC1.1-*Mmp13*, and pEPIC1.1-*Cxcl14* all induce strong over-expression compared to empty pEPIC1.1 (Fig. 1D–F). The pEPIC1.1-*Runx2* construct increased *Runx2* mRNA levels 27±4.3 times by qPCR (P<0.005) and RUNX2 protein levels 23±2.7 times by WB compared to pEPIC1.1 (P<0.005) (Fig. 1D). The pEPIC1.1-*Mmp13* construct increased *Mmp13* mRNA levels 480±2.4 times by qPCR (P<0.005) and the MMP13 protein levels 5±0.96 times by WB compared to pEPIC1.1 (P<0.005) (Fig. 1E). The pEPIC1.1-*Cxcl14* construct increased *Cxcl14* mRNA levels 59,000±16,000 times by qPCR (P<0.02) and the CXCL14 protein levels 32±4.6 times by WB compared to pEPIC1.1 (P<0.005) (Fig. 1F).

To confirm stable expression, we transfected DF-1 cells with pEPIC1.1 with or without pNano-hyPBase. Following transfection, cells were allowed to express GFP for 2 days to determine the baseline transfection efficiency. We then passaged the cells every 2 days for 20 days, to determine the stability of expression. We found that cells transfected without pNano-hyPBase rapidly lost GFP expression while those transfected with pNano-hyPBase initially had a small drop in GFP expression, which then stabilized over time. At 6 days post-transfection, cells with pNano-hyPBase retained higher levels of GFP expression compared to those without pNano-hyPBase (75%±5 compared to 35%±6, respectively, P<0.05) (Fig. 1G,H). By day 20, 70%±6 of cells transfected with pNano-hyPBase still expressed GFP, compared to <1% of cells without pNano-hyPBase.

We next confirmed that the pEPIC1.1 construct is functional at the tissue level. Mandibular primordia (i.e. 'mandibles') were dissected from HH24 chick embryos, injected with a plasmid solution containing pEPIC1.1-*Cxcl14* with or without hyPBase, and then electroporated. Mandibles were then cultured over 7 days. After 5 days of culture, mandibles electroporated with pNano-hyPBase retained strong GFP expression while mandibles without

Biology Open (2020) 9, bio055343. doi:10.1242/bio.055343

pNano-hyPBase had greatly reduced expression compared to 1-day post-electroporation (Fig. 1I). After 7 days of culture mandibles electroporated without pNano-hyPBase had no detectable GFP expression.

Generating the pPID2 *piggyBac* cloning vector

To enhance the versatility of our *piggyBac* vectors we generated a general *piggyBac* cloning vector pPID2 (*piggyBac*, insulator, DTS) (Fig. 2A). pPID2 uses the pNano backbone to maintain a minimal vector footprint and contains the enhanced *piggyBac* mutations (Lacoste et al., 2009), a DTS, insulator sequence, and a multicloning site with over 20 restriction enzyme sites including HindIII, PstI, SalI, XhoI, EcorI, PstI, NcoI, NgoMV, NheI, SpeI, MscI, and BglII, for ease of cloning.

When cells are transfected or electroporated with plasmids, transport from the cytoplasm to the nucleus is required for both expression and transposition into the genome. Plasmid entry into the nucleus generally occurs either during mitosis when the nuclear envelope breaks down, allowing for passive diffusion of plasmids into the nuclear space, or when the intracellular plasmid concentration is very high (10^4–10^6 molecules of plasmid DNA per cell) (Utvik et al., 1999; Young et al., 2003; Bai et al., 2017). To overcome potential nuclear import barriers, we added a DTS (Dean et al., 1999, 2005). A DTS functions by binding to transcription factors, which are then actively transported into the nucleus. We chose to use the simian virus 40 (SV40) 72 bp promoter DTS (Dean et al., 1999) because it can function in a wide variety of cell types (Dean, 1997; Young et al., 2003), is small, uses endogenously expressed transcription factors (Miller et al., 2009), and does not require expression of viral proteins (Dean et al., 2005). The DTS only directs plasmid entry into the nucleus and does not affect transgene localization. Alternatively, if nuclear entry is low even with a DTS, addition of trans-cyclohexane-1,2-diol reversibly increases the permeability of the nuclear pore complex allowing plasmids to diffuse into the nucleus (Vandenbroucke et al., 2007; De la Rossa and Jabaudon, 2015; Cervia et al., 2018).

Epigenetic and heterochromatic silencing of foreign DNA inserted into the host genome represent an obstacle for efficient transgene expression both at the time of insertion and over long-term expression (Garrison et al., 2007). Genomic insertions containing viral sequences are known to be actively silenced (Pannell and Ellis, 2001; Ellis, 2005; Wen et al., 2014; Hudecek et al., 2017). An insertion in a heterochromatic region or region that subsequently becomes heterochromatic may result in transgene inactivation (Janssen et al., 2018). To prevent this epigenetic silencing, we added a genetic insulator that blocks the spread of repressive epigenetic marks and heterochromatin (Ali et al., 2016). Moreover, insulator sequences help to protect endogenous sequences from epigenetic activation or silencing caused by the transposition (Hollister and Gaut, 2009). We used the D4Z4 insulator, which is only 65 bp and has been shown to efficiently protect *piggyBac* transgene expression (Ottaviani et al., 2009; Bire et al., 2013). pPID2 contains two D4Z4 insulator sequences contained within the *piggyBac* ITRs flanking the multicloning site (Fig. 2A).

Generating the pPIDNB doxycycline-inducible system

We also added a dox-inducible component to our over-expression constructs, which provides several advantages, including increased temporal control of expression. Without such precise temporal control, the premature and continuous expression of a gene of interest may disrupt development in ways that cause phenotypes unrelated to the processes under study. A dox-based strategy has several advantages over other inducible systems in that dox is extremely cheap and effective at low concentrations. Additionally, dox is able to diffuse efficiently through tissues allowing for induction past the surface level (Agwuh and MacGowan, 2006; Sato et al., 2007) and the use of dox-soaked beads or gels can allow for spatial control of expression.

We generated the pPIDNB (*piggyBac*, insulator, DTS, mNeonGreen, bi-directional) construct as a minimal dox-inducible plasmid (Fig. 2B). This plasmid is based upon the pPID2 backbone and includes the DTS, insulator, and *piggyBac* sequences. In addition, pPIDNB constitutively expresses the reverse tetracycline (tet) transactivator (rtTA) and mNeonGreen (GFP) under the PGK promoter (Shaner et al., 2013). The rtTA and mNeonGreen coding sequences are bicistronic and are separated by a porcine teschovirus-1 2A (P2A) site, which causes them to be expressed as two different peptide sequences (Szymczak et al., 2004; Kim et al., 2011). When bound to dox, the rtTA undergoes a conformational shift allowing binding and activation of the bidirectional tet promoter (Gossen et al., 1995; Das et al., 2016). We chose to use the rtTA-V16 variant of rtTA, which is both sensitive to dox and can induce strong expression (Das et al., 2016). Because the rtTA-V16 variant is under a constitutively active PGK promoter and not autoregulated, varying levels of dox can have a graded effect on gene expression at the cellular level rather than simply modulate expression like a binary switch (Herr et al., 2011; Heinz et al., 2013; Roney et al., 2016). On one side of the bidirectional promoter is mScarlet-I (RFP) serving as a marker for dox induction (Bindels et al., 2017). On the other side of the bi-directional promoter is the cloning site containing AflII and PsiI sites for dox-inducible expression of the gene of interest. Combining both the rtTA and tet promoter into a single construct enables stable inducible-expression with one integrating plasmid and one transposase-expressing plasmid. Moreover, for experiments that would benefit from the ability to detect nuclear localization, we also generated pPIDNB2, which has histone H2B fused to GFP to label nuclei (Bourgeois et al., 2015), in contrast to the pPIDNB plasmid where GFP localization is diffuse throughout the cell (Fig. 2C).

To evaluate the sensitivity of the pPIDNB plasmid to induction by dox, we transfected DF-1 cells and performed a dose-response analysis with dox for 24 h. In the absence of dox, there was a very low basal level of RFP expression, with only 0.15%±0.2% of the GFP positive cells also expressing detectable levels of RFP expression (Fig. 2D,E). After treating cells with 2.5 ng/ml dox, 52%±1.1% of the GFP positive cells also expressed RFP. We found that the percent of RFP expressing cells as a fraction of the GFP positive cells maxed out at a dose of 10 ng/ml dox at 88%±2.7% with cells treated at 50 ng/ml and 250 ng/ml dox expressing RFP at 80%±2.7% and 84%±7.3%, respectively (Fig. 2E). While the fraction of cells expressing RFP did not increase at dox concentrations greater than 10 ng/ml, the intensity of RFP did increase with higher concentrations of dox (Fig. 2D).

We next tested the ability of pPIDNB to drive exogenous gene expression by cloning in the coding sequences for *Cxcl14*, *Gas1* (a plasma membrane receptor, 945 bp), *Runx2*, and *Mmp13*. We first transfected DF-1 cells with pPIDNB-*Cxcl14*, treated with various doses of dox, and found that *Cxcl14* expression correlated with the concentration of dox (Fig. 2F). We found DF-1 cells treated with 2.5, 10, 50, and 250 ng/ml dox for 24 h increased *Cxcl14* mRNA expression by 27±6.4 (P<0.05), 96±23 (P<0.05), 149±34 (P<0.05), and 178±20 (P<0.005) times, respectively, compared to

Biology Open (2020) 9, bio055343. doi:10.1242/bio.055343

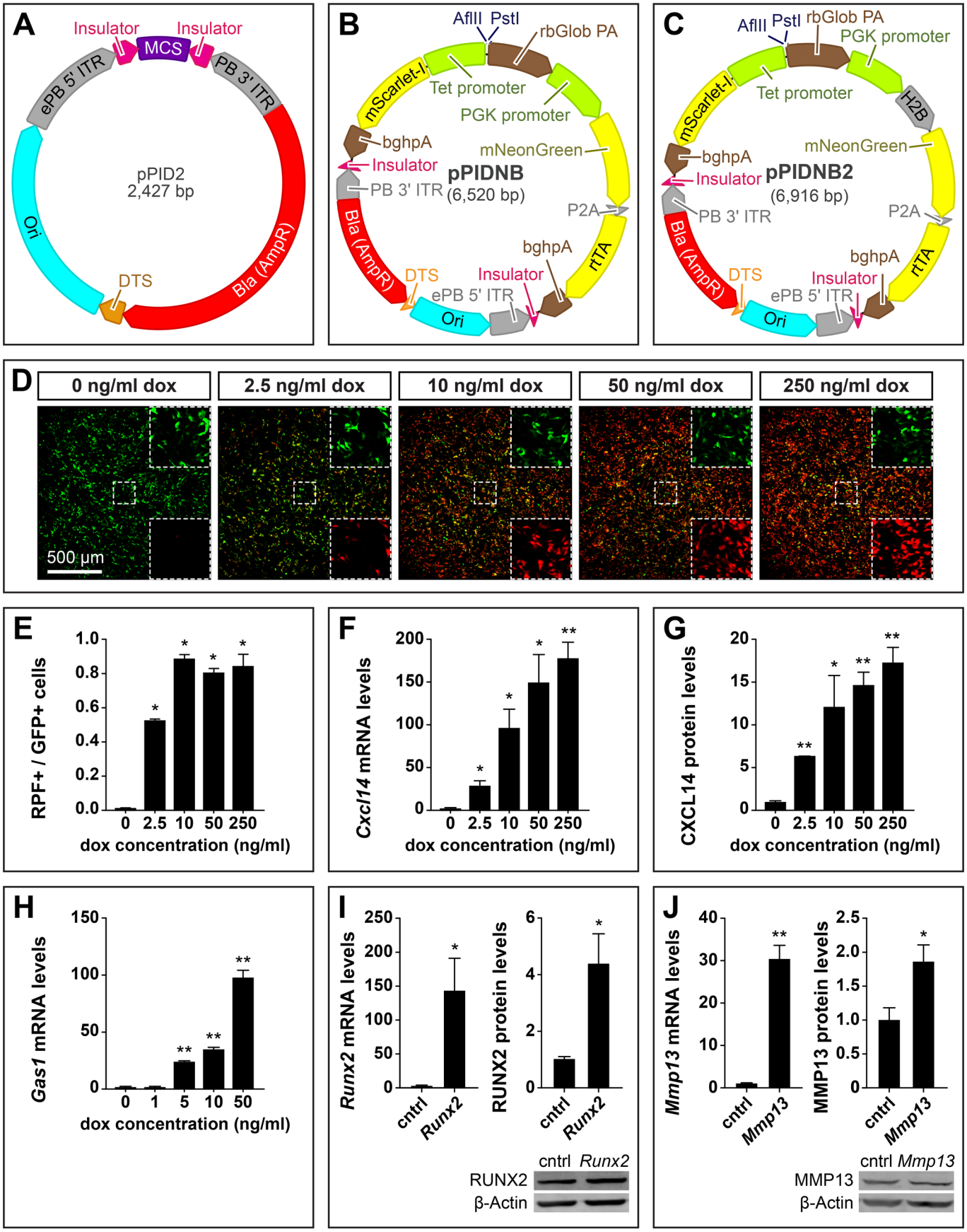

Fig. 2. See next page for legend.

Biology Open (2020) 9, bio055343. doi:10.1242/bio.055343

Fig. 2. Maps of doxycycline (dox)-inducible plasmids and over-expression analyses. (A) Map of the pPID2 *piggyBac* cloning vector showing insulators in magenta; a DTS in orange; MCS in purple; bacterial origin of replication (Ori) in cyan; bacterial β-lactamase (Bla) resistance gene (AmpR) in red; and *piggyBac* ITRs, IRES, and P2A sequences in grey. (B) Map of the pPIDNB *piggyBac* dox-inducible vector showing restriction sites for cloning, coding sequences in yellow, terminator sequences in brown, and promoter sequences in green. pPIDNB constitutively expresses mNeonGreen (GFP) and coding sequences can be cloned into the plasmid under a bidirectional tetracycline (tet) inducible promoter using the AflII and PstI restriction sites. mScarlet-I, a red fluorescent protein (RFP), is expressed on the alternate side of the bidirectional tet promoter. (C) Map of the pPIDNB2 vector, which is identical to pPIDNB except that GFP is localized to the nucleus using histone H2B. (D) DF-1 cells transfected with pPIDNB constitutively express GFP and differentially express RFP in response to varying concentrations of dox after 24 h. Higher resolution split channel image insets of the center area outlined by dashed lines show the GFP channel (top right) and RFP channel (bottom right). (E) RFP-positive (i.e. dox-induced) cells relative to total number of GFP-positive (i.e. transfected) cells. There were two biological replicates for each group. (F) Dox induction was measured in DF-1 cells on the mRNA level. There are three biological replicates for each group. (G) Dox dose response of protein levels for *Cxcl14*. There are three biological replicates for each group except for the 2.5 ng/ml treatment, which has two biological replicates. (H) Dox dose response of *Gas1* mRNA. There were four biological replicates for each group. Levels are relative to 0 ng/ml of dox and normalized to *18S* for mRNA and β-Actin for protein. (I) Over-expression of *Runx2* and (J) *Mmp13* with pPIDNB. DF-1 cells were transfected with control (cntrl) empty pPIDNB or pPIDNB plus *Runx2* or *Mmp13* coding sequence and treated with 50 ng/ml of dox for 24 h. mRNA levels were normalized using *18S* and protein using β-Actin. Representative WBs are shown below. There were four biological replicates for each group. All qPCRs were performed in technical duplicate. A two-tailed *t*-test was used for all statistical analyses. When multiple comparisons were made, *P*-values were adjusted using the Holm–Bonferroni method. All bar graphs are shown as mean±s.e.m. (**P*<0.05; ***P*<0.005).

cells not treated with dox (Fig. 2F). WB analysis also showed a dose response with 2.5, 10, 50, and 250 ng/ml dox with CXCL14 protein levels increasing by 6.3±0.053 (*P*<0.005), 12±3.8 (*P*<0.05), 15±1.6 (*P*<0.005), and 17±1.9 (*P*<0.005) times, respectively, compared to cells not treated with dox (Fig. 2G). These results in conjunction with the RFP data above suggest that dox dose-response is effectively tunable per unit cell and not simply a binary threshold response to increased dox concentrations that causes more cells to express RFP. These observations are consistent with previously published work demonstrating that varying the concentration of dox can have a graded effect on gene expression at the cellular level (Herr et al., 2011; Heinz et al., 2013; Roney et al., 2016).

To determine if pPIDNB can stably integrate into the genome and express a transgene, we transfected DF-1 cells with pPIDNB-*Gas1* and pNano-hyPBase. DF-1 cells were passaged over 4 weeks and then fluorescence-activated cell sorted (FACS) for GFP to confirm pPIDNB-*Gas1* could be stably integrated into the host genome and remain dox-inducible. We treated cells with dox and found that they were induced in a dose-response manner. After treating cells with 1, 5, 10, and 50 ng/ml dox for 24 h, *Gas1* mRNA expression increased by 1.1±0.16 (*P*>0.05), 23±0.99 (*P*<0.005), 34±2.7 (*P*<0.005), and 97±7.6 times (*P*<0.005), respectively, compared to cells not treated with dox (Fig. 2H). To confirm that pPIDNB can over-express different types of genes we also transfected DF-1 cells with either with empty pPIDNB, pPIDNB-*Runx2*, or pPIDNB-*Mmp13*. Transfected cells were treated with 50 ng/ml of dox for 24 h. The pPIDNB-*Runx2* and pPIDNB-*Mmp13* transfected cells expressed 140±47 (*P*<0.05) times more *Runx2* mRNA and 30±3.2 (*P*<0.005) times more *Mmp13* mRNA than cells transfected with empty pPIDNB, respectively (Fig. 2I,J). WB analyses also showed over-expression with pPIDNB-*Runx2* and pPIDNB-M*mp13* expressing 4.4±1.1 (*P*<0.05) and 1.9±0.25 (*P*<0.05) times more RUNX2 and MMP13 protein than pPIDNB alone, respectively.

Even though we found that 10 ng/ml of dox provides for high levels of induction, in order to achieve prolonged and robust gene expression in our subsequent long-term experiments, we decided to use 50 ng/ml dox. This higher concentration takes into account the half-life of dox, which is between 24–48 h in culture (based on estimates from the manufacturer), and our need to maintain gene expression for extended periods of time (like up to 10 days) without having to re-introduce additional dox, especially *in ovo*, so that we can minimize the number of times we handle samples.

Spatiotemporal control of expression in cell culture

To confirm that we could exert spatiotemporal control over transgene expression using pPIDNB, DF-1 cells were transfected with pNano-hyPBase and either pPIDNB-*Gas1* or pPIDNB2-*Gas1*. Cells were passaged for 4 weeks and then sorted for GFP to generate stable lines with either pPIDNB-*Gas1* or pPIDNB2-*Gas1* integrated into their genomes. Cells with integrated pPIDNB-*Gas1* or pPIDNB2-*Gas1* were visualized by GFP. pPIDNB-*Gas1* cells showed GFP localized throughout the entire cell while pPIDNB2-*Gas1* showed nuclear localization of GFP (Fig. 3A,B). Cells were then treated with 50 ng/ml dox and imaged at 0, 6, and 12 h post-dox treatment. After 6 h of dox treatment, cells began to express detectable levels of RFP and by 12 h the RFP signal was robust.

To determine if we could control the spatial localization of transgene expression, we applied minocycline microspheres to DF-1 cells transfected with pPIDNB-*Gas1*. These microspheres slowly release minocycline, a tetracycline (dox) analog, and induce the tet expression system (Chtarto et al., 2003; Zhou et al., 2006). We applied minocycline microspheres directly to a localized area in the well and cells were imaged at 0, 6, and 12 h after treatment. After 6 h, we observed low levels of RFP expression, and after 12 h RFP expression levels were high in areas adjacent to the microspheres but not in areas further away (Fig. 3C).

For experiments that could benefit from the ability to monitor dynamic changes in the cell cycle, we added a DNA helicase B (DHB) cell cycle sensor sequence (Spencer et al., 2013; Kohrman et al., 2020) to the dox-inducible RFP of pPIDNB2. The DHB cell cycle sensor translocates to the nucleus at G0/G1. During S phase, DHB localizes to both the nucleus and the cytoplasm and during M-phase DHB primarily localizes to the cytoplasm. The nuclear localization of GFP in pPIDNB2 allows for the determination of how much of the DHB signal is nuclear versus cytoplasmic. We transfected DF-1 cells with pPIDNB2 DHB and treated them with 50 ng/ml of dox and imaged them after 12 h. We found that we could identify cells in different phases of the cell cycle with nuclear-localized DHB (G0/G1), nuclear- and cytoplasm-localized DHB (S phase), and cytoplasm localized DHB (M phase) (Fig. 3D).

Temporal and spatial control of gene expression during development

To exert spatiotemporal control over gene expression in embryonic tissues, we unilaterally electroporated the presumptive cephalic NCM of HH8.5 chick embryos with pPIDNB and pNano-hyPBase. At HH10, we assayed for the extent of electroporation by visualizing GFP-positive cells *in ovo* in migrating NCM destined for the mandibular primordia (Fig. 4A). These embryos were then incubated until HH30, at which point the mandibular primordia

Biology Open (2020) 9, bio055343. doi:10.1242/bio.055343

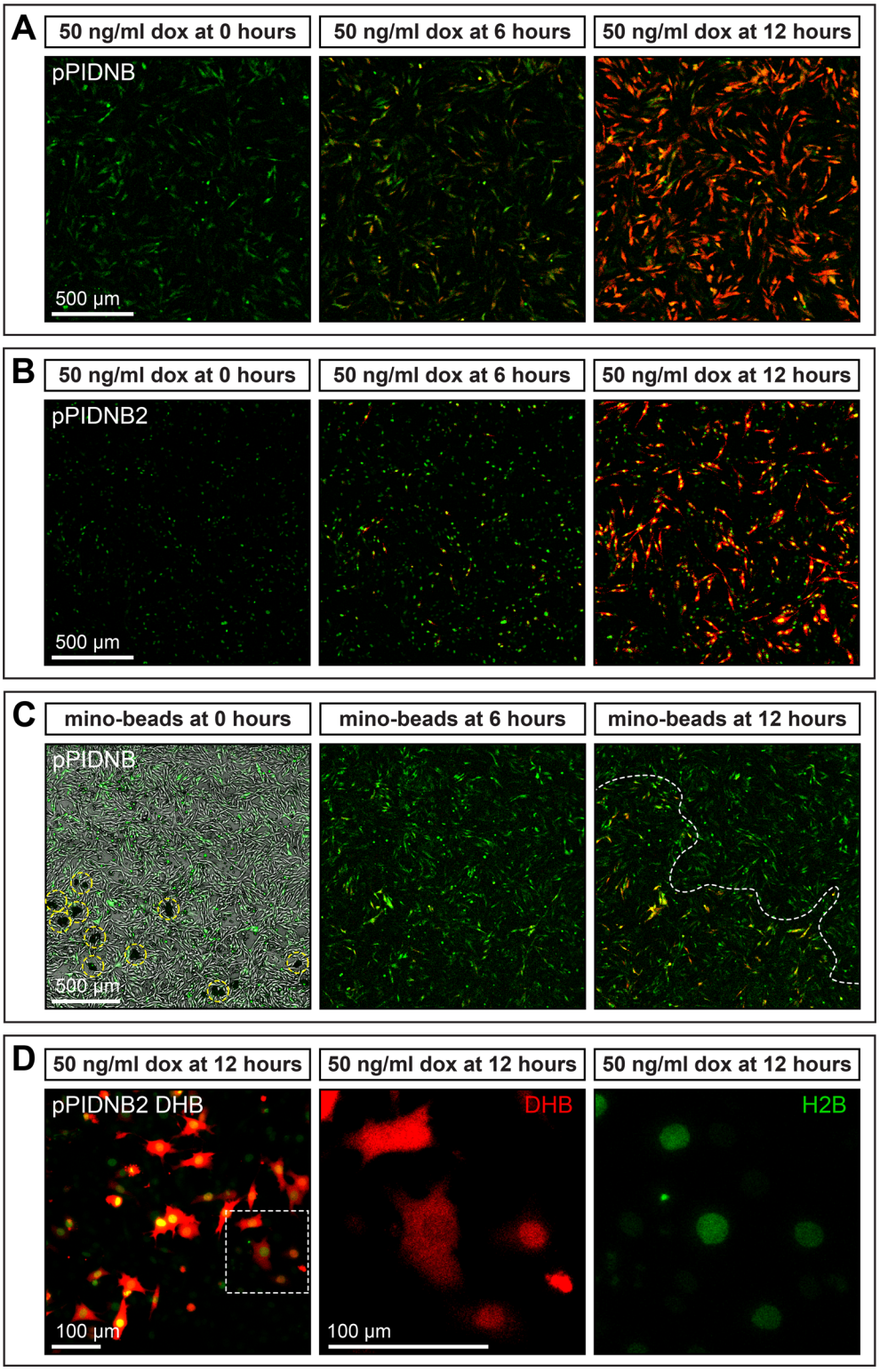

Fig. 3. *In vitro* induction of gene expression in cells. (A) DF-1 cells stably transfected with pPIDNB constitutively express mNeonGreen (GFP) and begin to express mScarlet-I (RFP) over time in response to treatment with 50 ng/ml doxycycline (dox). Cells were imaged at 0, 6, and 12 h post-treatment. (B) DF-1 cells stably transfected with pPIDNB2 constitutively express GFP in the nucleus and begin to express RFP over time in response to treatment with 50 ng/ml dox. Cells were imaged at 0, 6, and 12 h post-treatment. (C) DF-1 cells transfected with pPIDNB constitutively express GFP and begin to express RFP over time in response to treatment with minocycline microspheres. Cells were imaged at 0, 6, and 12 h post-treatment. Microspheres are circled in yellow and a boundary between cells that are induced versus those that are not is indicated by a white dashed line. (D) DF-1 cells transfected with pPIDNB2 DHB (DNA Helicase B) constitutively express GFP in the nucleus and the DHB cell cycle sensor is tagged with RFP and induced in response to 50 ng/ml dox as seen at 12 h post-treatment. White-dashed inset box indicates cells shown at higher magnification where RFP marks DHB localization and GFP marks nuclei. DHB localization appears enriched in the nucleus, cytoplasm, or diffused throughout the cell.

were dissected out, cultured with 50 ng/ml of dox, and imaged at 0, 12, and 24 h post-treatment. As evidence of the stable genomic integration and induction of the plasmids in embryos, we observe the electroporated side of the mandible expressing GFP, with the contralateral side showing little to no GFP expression. After 12 h, treatment with dox results in strong RFP signal that is co-localized with GFP and this RFP expression intensifies further by 24 h (Fig. 4A; Movie 1).

Additionally, some duck embryos were bilaterally electroporated at HH8.5 with pPIDNB-*Gas1* and pNano-hyPBase and were treated with 50 ng/ml dox *in ovo* at HH15. By HH24, we observed RFP expression throughout the mandibular primordia (Fig. 4B). To confirm that *in ovo* dox treatment would work efficiently even during later stages of development, some chick embryos were unilaterally electroporated at HH8.5 with pPIDNB and pNano-hyPBase, incubated for 7 days, and then were treated *in ovo* with a

Biology Open (2020) 9, bio055343. doi:10.1242/bio.055343

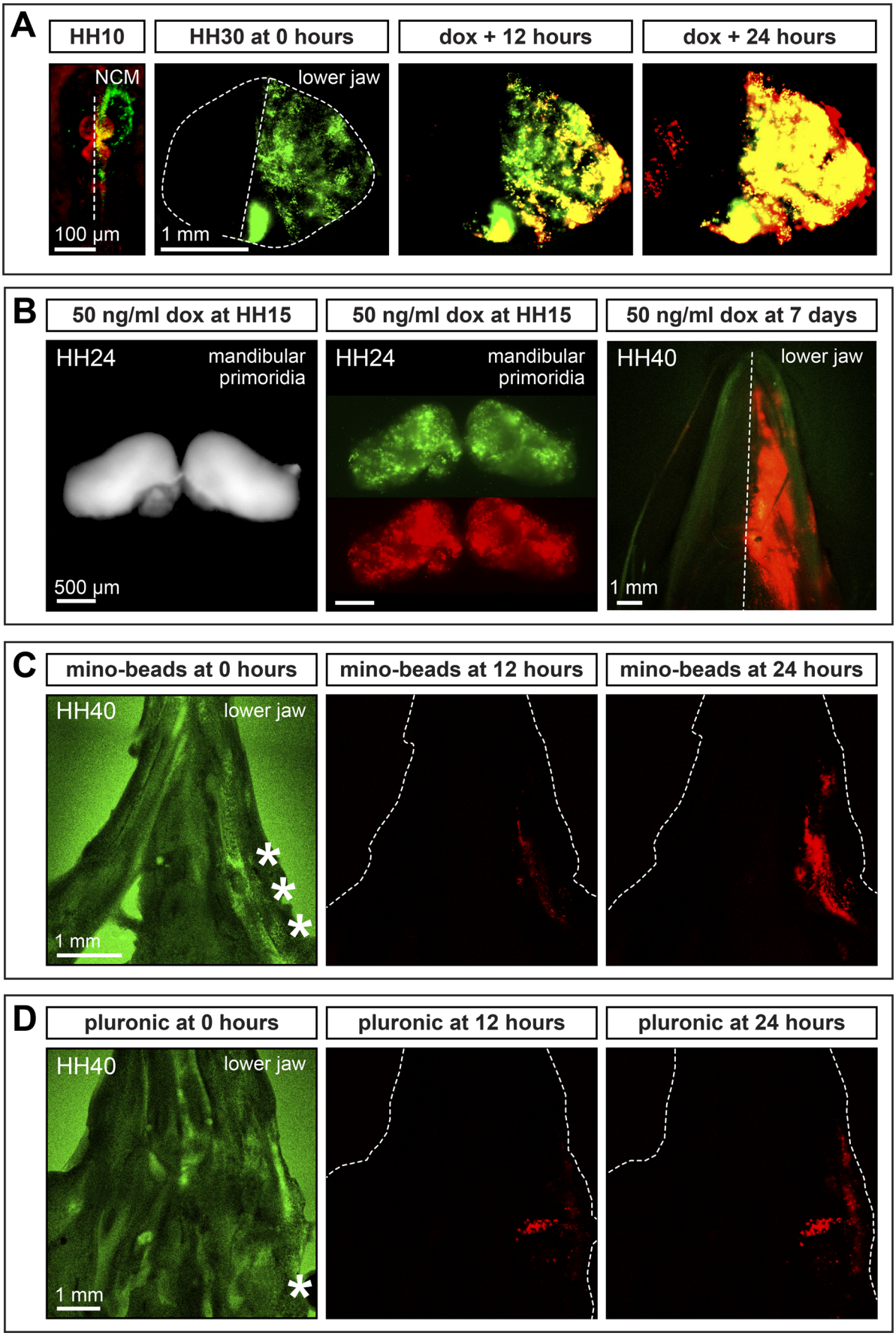

Fig. 4. See next page for legend.

Biology Open (2020) 9, bio055343. doi:10.1242/bio.055343

Fig. 4. *In ovo* and *ex vivo* induction of gene expression in the lower jaw. (A) Presumptive cephalic NCM electroporated unilaterally with pPIDNB and pNano-hyPBase in a chick embryo at HH8.5 constitutively expresses mNeonGreen (GFP) as shown at HH10 (counterstained red with neutral red). At HH30, the lower jaw shows unilateral GFP expression in NCM-derived tissues. After 12 and 24 h in culture, NCM express mScarlet (RFP) in response to treatment with 50 ng/ml doxycycline (dox). (B) Presumptive NCM bilaterally electroporated with pPIDNB and pNano-hyPBase in a duck embryo at HH8.5 shows RFP expression on both sides of the lower jaw at HH24 (after bilateral electroporation) when treated *in ovo* with 50 ng/ml dox at HH15. Presumptive NCM bilaterally electroporated with pPIDNB and pNano-hyPBase in a chick embryo at HH8.5 shows RFP expression on one side of the lower jaw at HH40 (after unilateral electroporation) when treated *in ovo* with 50 ng/ml dox 7 days after electroporation and imaged 9 days after treatment. (C) Presumptive NCM electroporated bilaterally with pPIDNB-*Gas1* and pNano-hyPBase in a duck embryo at HH8.5 shows RFP expression in the lower jaw (white dashed area) 12 and 24 h after being injected in culture with minocycline microspheres at HH40 (white asterisks). (D) Presumptive NCM electroporated unilaterally with pPIDNB-*Gas1* and pNano-hyPBase in a duck embryo at HH8.5 shows RFP expression in the lower jaw12 and 24 h after being treated at HH40 with 35% Pluronic F-127 gel containing 50 ng/ml dox (white asterisk). GFP and RFP channels shown at t=0. RFP channel shown for 12 and 24 h post-dox treatment. The margin of the lower jaw is represented by the white dashed line.

single dose of dox (50 ng/ml). These embryos were then allowed to develop for 9 more days (to around HH40), at which point we observed robust unilateral RFP expression in the lower jaw (Fig. 4B).

To exert more precise spatial control over gene expression, some embryos were bilaterally electroporated at HH8.5 with pPIDNB-*Gas1* and pNano-hyPBase and incubated until HH40. Their lower jaws were then harvested and either injected along the right side with minocycline microspheres or with dox gel (Pluronic F-127). Pluronic F-127 is a liquid at low temperatures (4°C) but solidifies at higher temperatures (37°C) and has been used for delivering drugs to different tissues (Harris et al., 2004; Giovagnoli et al., 2010). Whereas before treatment we observe GFP on both sides of the jaw, after 12 h of treatment with either minocycline microspheres or with dox gel, we observe RFP expression localized on the right side of the jaw, which becomes more elevated by 24 h (Fig. 4C,D).

Conclusion

In this study, we generated an 'all-in-one' *piggyBac* dox-inducible system. The pPIDNB plasmid is designed to be as small as possible to optimize cellular uptake while incorporating critical features to maximize its functionality. The DTS and insulator sequences serve to promote expression by directing nuclear entry of the plasmid and block heterochromatic silencing expression. We used mutated *piggyBac* and hyPBase sequences to increase genome integration efficiency. We have also incorporated a constitutively expressed GFP to mark cells that have taken in plasmid DNA and RFP to mark dox-induced cells. Our system facilitates precise temporal control of gene induction and is easily adapted for *in vitro* or *in ovo*. Spatial control of gene expression can be achieved by electroporating regions of interest and/or by applying beads or gels to localize the distribution of dox. This especially allows for electroporation of early avian embryos when ease of access and electroporation efficiency are highest. Embryos can then develop to their desired stage and the region of interest can be induced in a precise and rapid manner using dox-soaked beads or gel. Although we only tested induction in the lower jaw as a proof-of-concept, this same technique should be readily applicable to other accessible tissues in a developing avian embryo such as the limb buds, somites, neural tube, eyes, and heart.

The pPIDNB system is able to induce expression quickly and its reliance on a low dose of dox is important because dox has biological effects beyond antimicrobial activity including affecting matrix metalloproteinase activity, inflammation, the NF-κB pathway, and the nervous system (Bahrami et al., 2012; Alexander-Savino et al., 2016). High concentrations of dox (e.g. 1000 ng/ml) are cytotoxic in culture and have strong proliferative and metabolic effects, and some cell types are affected at even lower concentrations (e.g. 100–200 ng/ml) (Ermak et al., 2003; Ahler et al., 2013; Alexander-Savino et al., 2016). By using a low dose of dox (i.e. 50 ng/ml) we have likely minimized any off-target effects of dox treatment.

Based on the reasons described above, we were motivated to design the pPIDNB system even though other systems have been effective previously for achieving stable transgene expression in chick embryos. For example, *piggyBac* combined with heterologous promoters and *Cre/loxP* technology has enabled temporal control of transgene expression and cell-type-specific labeling in the neural tube (Lu et al., 2009). *Tol2*-based dox-inducible systems have also been generated (Sato et al., 2007; Watanabe et al., 2007; Takahashi et al., 2008) and applied to study NCM (Yokota et al., 2011). However, these systems require the integration of multiple plasmids in the same cell to function properly. While transposon integration is highly efficient, the likelihood of two or more different plasmids integrating is less than for a single plasmid. Our system only requires a single integrating plasmid, which both simplifies and improves the efficiency of electroporations. Another transposon-based integration method involves an 'integration-coupled On' (iOn) genetic switch, which has the advantage of being drug-free and limiting expression to productive transposition events (Kumamoto et al., 2020). However, in its current form the iOn system is not inducible at a given timepoint or location, which was a prerequisite for our experimental strategy. Specifically, for ongoing and future work, we want to electroporate NCM at HH8.5, perform transplants of electroporated NCM between quail and duck embryos at HH9.5, and then exert precise spatiotemporal control over transgene activation at HH34 or later by implanting beads that slowly and locally release dox. We imagine that equivalent approaches could be used to electroporate other avian tissues such as the somites for example at HH15 (Krull, 2004; Scaal et al., 2004; Pourquié, 2018), and then induce transgene expression in the developing limbs at any subsequent stage to investigate skeletal muscle patterning (Wang et al., 2011; Bourgeois et al., 2015).

While in the present study, we designed the pPIDNB construct for transgene over-expression, we envision that future applications will include different types of experiments such as gene knockdown using CRISPRi (Qi et al., 2013; Mandegar et al., 2016). For example, catalytically inactive *Cas9* could be placed with transcriptional repressors under an inducible tet promoter (Qi et al., 2013; Yeo et al., 2018). Constitutively active U6 promoters would drive expression of single guide RNAs (Cong et al., 2013; Gandhi et al., 2017; Williams et al., 2018). Using similar protocols for over-expression and knockdown would reduce the number of variables between experiments and help limit the confounding effects from different constructs. Overall, a great strength of avian model systems has been the combination of experimental embryology and modern genetic techniques. Our sensitive, stable, and robust inducible-promoter system builds on this strength and joins an arsenal of tools for manipulating gene expression in avians that will likely be useful to the broader community for addressing classic and current questions in developmental biology.

Biology Open (2020) 9, bio055343. doi:10.1242/bio.055343

MATERIALS AND METHODS

Plasmids

To generate pNano, the Ori and BlaR from pJet1.2 (Thermo Fisher Scientific, Waltham, MA, USA, K1231) were amplified using Q5 Hot Start High-Fidelity DNA Polymerase (NEB, Ipswich, MA, USA, M0493L). Fragments were cloned together using NEBuilder HiFi DNA Assembly Master Mix (NEB, Ipswich, MA, USA, E2621L). EcoRI, XhoI, and EcorV restriction enzyme sites were incorporated as tails added to the primers. To generate pEPIC1.1, the enhanced *piggyBac* ITRs, PGK promoter, 3× FLAG 2× Strep tag, IRES, mClover3, rabbit Beta globin terminator sequence, pNano were amplified by PCR using Q5 Hot Start High-Fidelity DNA Polymerase and cloned together using NEBuilder HiFi DNA Assembly Master Mix. The enhanced *piggyBac* ITRs were ordered as gBlocks (IDT, Coralville, IA, USA). The 3× FLAG 2× Strep tag sequence was amplified from AAVS1 Puro Tet3G 3× FLAG Twin Strep (Addgene, Watertown, MA, USA, 92099) (Dalvai et al., 2015). mClover3 sequence was amplified from pKanCMV-mClover3-mRuby3 (Addgene, Watertown, MA, USA, 74252) (Bajar et al., 2016). To generate pNano-hyPBase, the PGK promoter, hyPBase, and rabbit β-Globin poly A sequences were amplified by PCR using Q5 Hot Start High-Fidelity DNA Polymerase and cloned together using NEBuilder HiFi DNA Assembly Master Mix. To generate pPID2, the SV40 72 bp DTS and two 65 bp insulator sequences flanking MCS were ordered as gBlocks (IDT, Coralville, IA, USA). The enhanced *piggyBac* ITRs, Ori, and BlaR were amplified using Q5 Hot Start High-Fidelity DNA Polymerase and cloned together with the DTS and insulator gBlocks using NEBuilder HiFi DNA Assembly Master Mix. To generate pPIDNB, the bovine growth hormone poly A, mScarlet-I, bi-directional tet promoter, rabbit β-Globin poly A, PGK promoter, mNeonGreen P2A, and rtTA sequences were amplified by PCR using Q5 Hot Start High-Fidelity DNA Polymerase and then cloned together using NEBuilder HiFi DNA Assembly Master Mix. The bi-directional tet promoter and rtTA sequences were amplified from AAVS1 Puro Tet3G 3xFLAG Twin Strep (Addgene, Watertown, MA, USA, 92099). The mScarlet-I sequence was amplified from pmScarlet-i_C1 (Addgene, Watertown, MA, USA, 85044) (Bindels et al., 2017). To generate pPIDNB2, H2B was amplified using Q5 Hot Start High-Fidelity DNA Polymerase and then cloned into pPIDNB with QuikChange (Liu and Naismith, 2008) using KOD Xtreme Hot Start DNA Polymerase (MilliporeSigma, Burlington, MA, USA, 71975-3). To generate pPIDNB2-DHB, DHB was ordered as a gBlock and cloned into pPIDNB2 digested with XhoI (NEB, Ipswich, MA, USA, R0146S) and NotI (NEB, Ipswich, MA, USA, R3189S).

RNA extractions

For *Runx2*, *Mmp13*, and *Cxcl14*, RNA was extracted from DF-1 cells and HH27 whole chick heads using the RNeasy Plus Kit (Qiagen, Hilden, Germany, 74136) following the manufacturer's directions. Whole heads and DF-1 cells were resuspended in 600 µl of RTL plus buffer supplemented with 1% β-mercaptoethanol. Homogenization was carried out in a Bead Mill 24 (Thermo Fisher Scientific, Waltham, MA, USA, 15-340-163) at 5 m/s for 30 s. Following purification of total RNA, residual genomic DNA was removed using TURBO DNA-free Kit (Invitrogen, Carlsbad, CA, USA, AM1907). For RNA extractions involving *Gas1*, the PicoPure RNA Isolation Kit (Applied Biosystems, Foster City, CA, USA, KIT0204) was used following the manufacturer's directions and homogenization was carried out in a Bead Mill 24 (Fisher Scientific Waltham, MA, USA, 15-340-163) at 4 m/s for 15 s.

Cloning coding sequences

Full length cDNA synthesis from RNA was carried out using Maxima H-reverse transcriptase (Thermo Fisher Scientific, Waltham, MA, USA, K1651) following the manufacturer's directions with 2 µg of total RNA and 100 pmol of d(T)20 VN primer. The cDNA synthesis reaction was carried out at 50°C for 30 min, 55°C for 10 min, 60°C for 10 min, 65°C for 10 min, and 85°C for 5 min. Full length *Runx2*, *Mmp13*, *Cxcl14*, and *Gas1* were amplified by PCR using Q5 Hot Start High-Fidelity DNA Polymerase (NEB, Ipswich, MA, USA, M0493L) and cloned using CloneJET PCR Cloning Kit (Thermo Fisher Scientific, Waltham, MA, USA, K1231). Following confirmation of cloning of full length coding sequences by Sanger sequencing, *Runx2*, *Mmp13*, *Cxcl14*, and *Gas1* were cloned into pEPIC1.1 digested with AflII (NEB, Ipswich, MA, USA, R0520S) and EcoRI (NEB, Ipswich, MA, USA, R3101S) or pPIDNB digested with AflII (NEB, Ipswich, MA, USA, R0520S) and PstI (NEB, Ipswich, MA, USA, R3140S) using NEBuilder HiFi DNA Assembly Master Mix. All constructs were verified by Sanger sequencing and midipreped for electroporation and transfection using PureLink Fast Low-Endotoxin Midi Kit (Invitrogen, Carlsbad, CA, USA, A36227).

Avian embryos and cell culture

Fertilized eggs of chicken (*Gallus gallus*) and duck (*Anas platyrhynchos*) were purchased from AA Lab Eggs (Westminster, CA, USA) and incubated at 37.5°C in a humidified chamber (GQF Hova-Bator, Savannah, GA, USA, 1588) until they reached embryonic stages appropriate for manipulation and/or analyses. For all experiments, we adhered to accepted practices for the humane treatment of avian embryos as described in S3.4.4 of the AVMA Guidelines for the Euthanasia of Animals: 2013 Edition (Leary et al., 2013). Embryos were matched at equivalent stages using the Hamburger and Hamilton (HH) staging system, a well-established standard which utilizes an approach based on external morphological characters and that is independent of body size and incubation time (Hamburger and Hamilton, 1951; Hamilton, 1965; Ricklefs and Starck, 1998; Starck and Ricklefs, 1998). For late embryonic stages, we relied primarily on growth of the limbs, facial primordia, feather buds, and eyes (Eames and Schneider, 2005, 2008; Merrill et al., 2008).

Embryonic chick fibroblasts (DF-1) were purchased (ATCC, Manassas, VA, USA, CRL-12203) and cultured in Dulbecco's Modified Eagle's Medium (DMEM, Corning, NY, USA, 10-013-CV) supplemented with 10% FBS (VWR, Radnor, PA, USA, 97068-085, Lot# 283K18) and 1× penicillin-streptomycin (Thermo Fisher Scientific, Waltham, MA, USA, 15140122) at 37°C with 5% CO_2. These cells were confirmed to be chicken cells via PCR and by sequencing *Runx2*. Cells were passaged twice a week and monitored for mycoplasma contamination every 4 weeks. Cells were transfected with lipofectamine 3000 (Thermo Fisher Scientific, Waltham, MA, USA, L3000008) according to the manufacturer's instructions. Transfections for integrating *piggyBac* vectors were carried out in six-well plates with 5 µg *piggyBac* plasmid, 5 µg of pNano-hyPBase, and 20 µl of P3000.

Electroporations

Electroporations were performed by injecting a solution of pEPIC1.1-Cxcl14 and pNano-hyPBase at 3 µg/µl and 1 µg/µl, respectively, with a small amount of Fast Green dye. DNA was injected with a Pneumatic PicoPump (World Precision Instruments, Sarasota County, FL, USA, PV830) into dissected HH21 mandibular primordia using thin wall borosilicate glass micropipettes (O.D. 1.0 mm, I.D. 0.75 mm, Sutter Instrument Company, Novato, CA, USA, B100-75-10) pulled on a micropipette puller (Sutter iInstrument Company, Novato, CA, USA, P-97 Flaming/Brown). Mandibles were placed between two gold plate electrodes 0.5 cm apart submerged in Hanks' balanced salt solution (HBSS, Thermo Fisher Scientific, Waltham, MA, USA, 14170120). Electroporations were carried out by delivering five square pulses at 25 V for 50 ms spaced 500 ms apart (CUY21EDITII Next Generation Electroporator, BEX CO, Ltd). Mandibles were then cultured in BgJB medium (Thermo Fisher Scientific, Waltham, MA, USA, 12591038) supplemented with 10% FBS (VWR, Radnor, PA, USA, 97068-085, Lot# 283K18) and 1× penicillin-streptomycin (Thermo Fisher Scientific, Waltham, MA, USA, 15140122).

In ovo electroporations were performed using a solution of pPIDNB and pNano-hyPBase at 3 µg/µl and 1 µg/µl, respectively. With the addition of Fast Green tracer dye, DNA solution was injected into HH8.5 chick neural tubes with a Pneumatic PicoPump using thin wall borosilicate glass micropipettes pulled on a micropipette puller. Platinum electrodes were positioned on each side of the area pellucida, centered along the neural folds of the midbrain-hindbrain boundary as done previously to target the presumptive NCM destined for the mandibular arch (Creuzet et al., 2002; Krull, 2004; McLennan and Kulesa, 2007; Hall et al., 2014). For unilateral electroporations, we delivered three square pulses at 50 V for 1 ms spaced 50 ms apart followed by five square pluses at 10 V for 50 ms spaced 50 ms

apart. For bilateral electroporations, we delivered three square pulses at 50 V for 1 ms spaced 50 ms apart, three square pulses at 50 V for 1 ms spaced 50 ms apart in the reverse polarity, five square pluses at 10 V for 50 ms spaced 50 ms apart followed by, five square pluses at 10 V for 50 ms spaced 50 ms apart in the reverse polarity.

qPCR

DNased RNA was reverse-transcribed using iSCRIPT (Bio-Rad, Hercules, CA, USA, 1708841). Gene expression was quantified by qPCR with iQ SYBR Green Supermix (Bio-Rad, Hercules, CA, USA, 1708882) and normalized to 18S rRNA following previously published protocols (Dole et al., 2015; Smith et al., 2016). Primer sets were designed and optimized as described previously (Ealba and Schneider, 2013) and are listed in Table S1. Each sample was assayed in technical duplicate.

Western blot

DF-1 cells were lysed with 1× RIPA lysis buffer (MilliporeSigma, Burlington, MA, USA, 20-188) containing Halt protease inhibitors (Thermo Fisher Scientific, Waltham, MA, USA, 78430). A BCA assay (Thermo Fisher Scientific, Waltham, MA, USA, 23225) using a SpectraMax M5 plate reader (Molecular Devices, San Jose, CA, USA) was performed to quantify protein, and 40 µg protein was electrophoresed on a 10% SDS polyacrylamide gel following a published protocol (Smith et al., 2016). Proteins were transferred to an Imobilon-PVDF membrane (MilliporeSigma, Burlington, MA, USA, IPVH00010). Membranes were probed with rabbit anti-chick RUNX2 primary antibody (1:1000, Abcam Burlingame, CA, USA, #ab23981), custom made rabbit anti-chick MMP13 antibody (1 µg/ml, GenScript, Piscataway, NJ, USA), rabbit anti-CXCL14 (0.2 µg/ml, PeproTech, Rocky Hill, NJ, USA, 500-P237), mouse anti-chick β-actin antibody (1:4000, Novus Biologicals, Littleton, CO, USA, NB600-501), goat anti-rabbit IRDye 800CW (1:15000, LI-COR, Lincoln, NE, USA, 925-32211), and donkey anti-mouse IRDye 680RD antibody (1:15,000, LI-COR, Lincoln, NE, USA, 925-68072). Fluorescent signal was captured using the Odyssey Imaging System (Thermo Fisher Scientific, Waltham, MA, USA). Quantifications of protein bands were performed using Image Studio Lite. RUNX2, MMP13, and CXCL14 levels were normalized to β-actin.

Doxycycline treatment

Stock solutions of doxycycline hyclate (Acros Organics, Fair Lawn, NJ, USA, 446060250) were made to a final concentration of 1 mg/ml in water, filter sterilized, and stored at −20°C as single use aliquots. DF-1 cells and mandibles were treated in culture with the stock solution diluted in DMEM, with minocycline microspheres (Arrestin) added directly to each well, or by suspending microspheres in PBS and injecting them into the lower jaw with a 30-gauge needle. Pluronic F-127 (MilliporeSigma, Burlington, MA, USA, P2443-250G) was dissolved at a final concentration of 35% (w/v) in DMEM growth medium rocking at 4°C for 48 h. Dox was added to Pluronic F-127 for a final concentration of 500 ng/ml and injected into the lower jaw with an 18-gauge needle. For *in ovo* treatments, 2.5 µl (for chick) and 3.75 µl (for duck) of the 1 mg/ml dox stock solution was diluted with 750 µl of HBSS. This solution was then gently pipetted into the egg adjacent to the embryo and allowed to diffuse.

Imaging

DF-1 cells were imaged using a macroconfocal (Nikon, Minato City, Tokyo, Japan, AZ100 C2+). Time-lapse experiments were carried out in a custom-made stage top incubator (Okolab, Ambridge, PA, USA) set to 37°C, 95% humidity and 5% CO_2. All DF-1 experiments were carried out in six-well plates (Corning, Corning, NY, USA, 08-772-1B) with 2 ml of DMEM. Lower jaw time-lapse experiments were carried out on six-well transwell membranes (VWR, Radnor, PA, USA, 10769-192) with 2 ml of DMEM. Brightfield and fluorescent images of duck HH24 mandibular primordia were captured on an epifluorescent stereomicroscope (Leica, Wetzlar, Germany, MZFLIII).

Fluorescence-activated cell sorting (FACS)

DF-1 cells were washed with 2 ml of Trypsin followed by 3mL fresh wash. Trypsin activity was inhibited by adding 5 ml of DMEM with 10% FBS. Cells were pipetted and passed through 70 µm filter. Cells were sorted on FACSAriaII Flow Cytometer (BD Biosciences, San Jose, CA, USA). For all sorts, debris and dead cells were eliminated using FSC-A and SSC-A gating, doublets were excluded via gating discrimination using FSC-H and FSC-W, and only GFP+ cells were collected.

Statistical analysis

Statistical analysis carried out using Student's *t*-test was performed (GraphPad Prism version 8.4.3, GraphPad Software, La Jolla, CA, USA). When multiple comparisons were made, *P*-values were adjusted using the Holm–Bonferroni method (Holm, 1979). We aimed to have at least three biological replicates for each experiment.

Acknowledgements

We thank Tony Qu, Austen Lucena, Paul Asfour, Kate Woronowicz, and Jessye Aggleton for laboratory assistance and/or comments on the manuscript; T. Dam at AA Lab Eggs for fertilized chick and duck eggs; and the UCSF Biological Imaging Development Core (BIDC) for microscopy support. The pmScarlet-i_C1 was a gift from Dorus Gadella (Addgene, #85044). The AAVS1 Puro Tet3G 3xFLAG Twin Strep was a gift from Yannick Doyon (Addgene, # 92099). The pKanCMV-mClover3-mRuby3 was a gift from Michael Lin (Addgene, #74252). The pCAG-Cre-IRES2-GFP was a gift from Anjen Chenn (Addgene, #26646). The pCMV-hyPBase was provided by the Wellcome Trust Sanger Institute. The mNeonGreen was provided by Allele Biotechnology & Pharmaceuticals. The DHB was a gift from Dave Matus. The PGK promoter was a gift from Jonathan Brunger via Tamara Alliston.

Competing interests

The authors declare no competing or financial interests.

Author contributions

Conceptualization: R.A.S.; Methodology: D.C.; Validation: D.C., A.N., S.S.S., Z.V.; Formal analysis: D.C., A.N., S.S.S., Z.V.; Investigation: D.C., A.N., S.S.S., Z.V.; Resources: D.C.; Writing - original draft: D.C., R.A.S.; Writing - review & editing: D.C., A.N., S.S.S., Z.V., R.A.S.; Visualization: D.C., A.N., S.S.S., Z.V., R.A.S.; Supervision: R.A.S.; Project administration: R.A.S.; Funding acquisition: R.A.S.

Funding

This work was supported in part by National Institutes of Health (NIH)/National Institute for Dental Research (NIDCR) F30 DE027616 to A.N.; F31 DE027283 to S.S.S.; and R01 DE016402, R01 DE025668, and Office of the Director S10 OD021664 to R.A.S.

Data availability

Datasets supporting the results of this study are available upon reasonable request from the corresponding author (R.A.S.). Plasmids are also available upon request subject to the terms of the original licenses under which they were obtained. GenBank accession numbers for nucleotide sequences are as follows: Runx2 (MW036689), Mmp13 (MW036690), Gas1 (MW036691), and Cxcl14 (MW036692).

Supplementary information

Supplementary information available online at
https://bio.biologists.org/lookup/doi/10.1242/bio.055343.supplemental

References

Abramyan, J. and Richman, J. M. (2018). Craniofacial development: discoveries made in the chicken embryo. *Int. J. Dev. Biol.* **62**, 97-107. doi:10.1387/ijdb.170321ja

Agwuh, K. N. and MacGowan, A. (2006). Pharmacokinetics and pharmacodynamics of the tetracyclines including glycylcyclines. *J. Antimicrob. Chemother.* **58**, 256-265. doi:10.1093/jac/dkl224

Ahler, E., Sullivan, W. J., Cass, A., Braas, D., York, A. G., Bensinger, S. J., Graeber, T. G. and Christofk, H. R. (2013). Doxycycline alters metabolism and proliferation of human cell lines. *PLoS ONE* **8**, e64561. doi:10.1371/journal.pone.0064561

Ahn, J., Lee, J., Park, J. Y., Oh, K. B., Hwang, S., Lee, C.-W. and Lee, K. (2017). Targeted genome editing in a quail cell line using a customized CRISPR/Cas9 system. *Poult. Sci.* **96**, 1445-1450. doi:10.3382/ps/pew435

Alexander-Savino, C. V., Hayden, M. S., Richardson, C., Zhao, J. and Poligone, B. (2016). Doxycycline is an NF-κB inhibitor that induces apoptotic cell death in malignant T-cells. *Oncotarget* **7**, 75954-75967. doi:10.18632/oncotarget.12488

Ali, T., Renkawitz, R. and Bartkuhn, M. (2016). Insulators and domains of gene expression. *Curr. Opin. Genet. Dev.* **37**, 17-26. doi:10.1016/j.gde.2015.11.009

Bahrami, F., Morris, D. L. and Pourgholami, M. H. (2012). Tetracyclines: drugs with huge therapeutic potential. *Mini Rev. Med. Chem.* **12**, 44-52. doi:10.2174/138955712798868977
Bai, H., Lester, G. M. S., Petishnok, L. C. and Dean, D. A. (2017). Cytoplasmic transport and nuclear import of plasmid DNA. *Biosci. Rep.* **37**, BSR20160616. doi:10.1042/BSR20160616
Bajar, B. T., Wang, E. S., Lam, A. J., Kim, B. B., Jacobs, C. L., Howe, E. S., Davidson, M. W., Lin, M. Z. and Chu, J. (2016). Improving brightness and photostability of green and red fluorescent proteins for live cell imaging and FRET reporting. *Sci. Rep.* **6**, 20889. doi:10.1038/srep20889
Bednarczyk, M., Kozłowska, I., Łakota, P., Szczerba, A., Stadnicka, K. and Kuwana, T. (2018). Generation of transgenic chickens by the non-viral, cell-based method: effectiveness of some elements of this strategy. *J. Appl. Genet.* **59**, 81-89. doi:10.1007/s13353-018-0429-6
Betancur, P., Bronner-Fraser, M. and Sauka-Spengler, T. (2010). Assembling neural crest regulatory circuits into a gene regulatory network. *Annu. Rev. Cell Dev. Biol.* **26**, 581-603. doi:10.1146/annurev.cellbio.042308.113245
Bindels, D. S., Haarbosch, L., van Weeren, L., Postma, M., Wiese, K. E., Mastop, M., Aumonier, S., Gotthard, G., Royant, A., Hink, M. A. et al. (2017). mScarlet: a bright monomeric red fluorescent protein for cellular imaging. *Nat. Methods* **14**, 53-56. doi:10.1038/nmeth.4074
Bire, S., Gosset, D., Jégot, G., Midoux, P., Pichon, C. and Rouleux-Bonnin, F. (2013). Exogenous mRNA delivery and bioavailability in gene transfer mediated by piggyBac transposition. *BMC Biotechnol.* **13**, 75. doi:10.1186/1472-6750-13-75
Bochkov, Y. A. and Palmenberg, A. C. (2006). Translational efficiency of EMCV IRES in bicistronic vectors is dependent upon IRES sequence and gene location. *BioTechniques* **41**, 283-284, 286, 288 passim. doi:10.2144/000112243
Bourgeois, A., Esteves de Lima, J., Charvet, B., Kawakami, K., Stricker, S. and Duprez, D. (2015). Stable and bicistronic expression of two genes in somite- and lateral plate-derived tissues to study chick limb development. *BMC Dev. Biol.* **15**, 39. doi:10.1186/s12861-015-0088-3
Bower, D. V., Sato, Y. and Lansford, R. (2011). Dynamic lineage analysis of embryonic morphogenesis using transgenic quail and 4D multispectral imaging. *Genesis* **49**, 619-643. doi:10.1002/dvg.20754
Bronner-Fraser, M. (1996). Manipulations of neural crest cells or their migratory pathways. *Methods Cell Biol.* **51**, 61-79. doi:10.1016/S0091-679X(08)60622-6
Bronner-Fraser, M. and Garcia-Castro, M. (2008). Manipulations of neural crest cells or their migratory pathways. *Methods Cell Biol.* **87**, 75-96. doi:10.1016/S0091-679X(08)00204-5
Brooks, A. R., Harkins, R. N., Wang, P., Qian, H. S., Liu, P. and Rubanyi, G. M. (2004). Transcriptional silencing is associated with extensive methylation of the CMV promoter following adenoviral gene delivery to muscle. *J. Gene Med.* **6**, 395-404. doi:10.1002/jgm.516
Cerny, R., Lwigale, P., Ericsson, R., Meulemans, D., Epperlein, H.-H. and Bronner-Fraser, M. (2004). Developmental origins and evolution of jaws: new interpretation of "maxillary" and "mandibular". *Dev. Biol.* **276**, 225-236. doi:10.1016/j.ydbio.2004.08.046
Cervia, L. D., Chang, C.-C., Wang, L., Mao, M. and Yuan, F. (2018). Enhancing electrotransfection efficiency through improvement in nuclear entry of plasmid DNA. *Mol. Ther. Nucleic Acids* **11**, 263-271. doi:10.1016/j.omtn.2018.02.009
Chapman, S. C., Lawson, A., Macarthur, W. C., Wiese, R. J., Loechel, R. H., Burgos-Trinidad, M., Wakefield, J. K., Ramabhadran, R., Mauch, T. J. and Schoenwolf, G. C. (2005). Ubiquitous GFP expression in transgenic chickens using a lentiviral vector. *Development* **132**, 935-940. doi:10.1242/dev.01652
Chen, C.-M. A., Smith, D. M., Peters, M. A., Samson, M. E. S., Zitz, J., Tabin, C. J. and Cepko, C. L. (1999). Production and design of more effective avian replication-incompetent retroviral vectors. *Dev. Biol.* **214**, 370-384. doi:10.1006/dbio.1999.9432
Chen, Y. X., Krull, C. E. and Reneker, L. W. (2004). Targeted gene expression in the chicken eye by in ovo electroporation. *Mol. Vis.* **10**, 874-883.
Chesnutt, C. and Niswander, L. (2004). Plasmid-based short-hairpin RNA interference in the chicken embryo. *Genesis* **39**, 73-78. doi:10.1002/gene.20028
Chtarto, A., Tenenbaum, L., Velu, T., Brotchi, J., Levivier, M. and Blum, D. (2003). Minocycline-induced activation of tetracycline-responsive promoter. *Neurosci. Lett.* **352**, 155-158. doi:10.1016/j.neulet.2003.08.067
Clarke, J. D. W. and Tickle, C. (1999). Fate maps old and new. *Nat. Cell Biol.* **1**, E103-E109. doi:10.1038/12105
Cong, L., Ran, F. A., Cox, D., Lin, S., Barretto, R., Habib, N., Hsu, P. D., Wu, X., Jiang, W., Marraffini, L. A. et al. (2013). Multiplex genome engineering using CRISPR/Cas systems. *Science* **339**, 819-823. doi:10.1126/science.1231143
Creuzet, S., Couly, G., Vincent, C. and Le Douarin, N. M. (2002). Negative effect of Hox gene expression on the development of the neural crest-derived facial skeleton. *Development* **129**, 4301-4313.
Curcio, M. J. and Derbyshire, K. M. (2003). The outs and ins of transposition: from mu to kangaroo. *Nat. Rev. Mol. Cell Biol.* **4**, 865-877. doi:10.1038/nrm1241
Dalvai, M., Loehr, J., Jacquet, K., Huard, C. C., Roques, C., Herst, P., Côté, J. and Doyon, Y. (2015). A scalable genome-editing-based approach for mapping multiprotein complexes in human cells. *Cell Rep.* **13**, 621-633. doi:10.1016/j.celrep.2015.09.009
Das, R. M., Van Hateren, N. J., Howell, G. R., Farrell, E. R., Bangs, F. K., Porteous, V. C., Manning, E. M., McGrew, M. J., Ohyama, K., Sacco, M. A. et al. (2006). A robust system for RNA interference in the chicken using a modified microRNA operon. *Dev. Biol.* **294**, 554-563. doi:10.1016/j.ydbio.2006.02.020
Das, A. T., Tenenbaum, L. and Berkhout, B. (2016). Tet-on systems for doxycycline-inducible gene expression. *Curr. Gene Ther.* **16**, 156-167. doi:10.2174/1566523216666160524144041
De la Rossa, A. and Jabaudon, D. (2015). In vivo rapid gene delivery into postmitotic neocortical neurons using iontoporation. *Nat. Protoc.* **10**, 25-32. doi:10.1038/nprot.2015.001
Dean, D. A. (1997). Import of plasmid DNA into the nucleus is sequence specific. *Exp. Cell Res.* **230**, 293-302. doi:10.1006/excr.1996.3427
Dean, D. A., Dean, B. S., Muller, S. and Smith, L. C. (1999). Sequence requirements for plasmid nuclear import. *Exp. Cell Res.* **253**, 713-722. doi:10.1006/excr.1999.4716
Dean, D. A., Strong, D. D. and Zimmer, W. E. (2005). Nuclear entry of nonviral vectors. *Gene Ther.* **12**, 881-890. doi:10.1038/sj.gt.3302534
Ding, S., Wu, X., Li, G., Han, M., Zhuang, Y. and Xu, T. (2005). Efficient transposition of the piggyBac (PB) transposon in mammalian cells and mice. *Cell* **122**, 473-483. doi:10.1016/j.cell.2005.07.013
Dole, N. S., Kapinas, K., Kessler, C. B., Yee, S.-P., Adams, D. J., Pereira, R. C. and Delany, A. M. (2015). A single nucleotide polymorphism in osteonectin 3′ untranslated region regulates bone volume and is targeted by miR-433. *J. Bone Miner. Res.* **30**, 723-732. doi:10.1002/jbmr.2378
Ealba, E. L. and Schneider, R. A. (2013). A simple PCR-based strategy for estimating species-specific contributions in chimeras and xenografts. *Development* **140**, 3062-3068. doi:10.1242/dev.092676
Ealba, E. L., Jheon, A. H., Hall, J., Curantz, C., Butcher, K. D. and Schneider, R. A. (2015). Neural crest-mediated bone resorption is a determinant of species-specific jaw length. *Dev. Biol.*. **408**, 151-163. doi:10.1016/j.ydbio.2015.10.001
Eames, B. F. and Schneider, R. A. (2005). Quail-duck chimeras reveal spatiotemporal plasticity in molecular and histogenic programs of cranial feather development. *Development* **132**, 1499-1509. doi:10.1242/dev.01719
Eames, B. F. and Schneider, R. A. (2008). The genesis of cartilage size and shape during development and evolution. *Development* **135**, 3947-3958. doi:10.1242/dev.023309
Ellis, J. (2005). Silencing and variegation of gammaretrovirus and lentivirus vectors. *Hum. Gene. Ther.* **16**, 1241-1246. doi:10.1089/hum.2005.16.1241
Ermak, G., Cancasci, V. J. and Davies, K. J. A. (2003). Cytotoxic effect of doxycycline and its implications for tet-on gene expression systems. *Anal. Biochem.* **318**, 152-154. doi:10.1016/S0003-2697(03)00166-0
Fekete, D. M. and Cepko, C. L. (1993a). Replication-competent retroviral vectors encoding alkaline phosphatase reveal spatial restriction of viral gene expression/transduction in the chick embryo. *Mol. Cell. Biol.* **13**, 2604-2613. doi:10.1128/MCB.13.4.2604
Fekete, D. M. and Cepko, C. L. (1993b). Retroviral infection coupled with tissue transplantation limits gene transfer in the chicken embryo. *Proc. Natl. Acad. Sci. USA* **90**, 2350-2354. doi:10.1073/pnas.90.6.2350
Fish, J. L. and Schneider, R. A. (2014). Assessing species-specific contributions to craniofacial development using quail-duck chimeras. *J. Vis. Exp.* **87**, 1-6. doi:10.3791/51534
Fish, J. L., Sklar, R. S., Woronowicz, K. C. and Schneider, R. A. (2014). Multiple developmental mechanisms regulate species-specific jaw size. *Development* **141**, 674-684. doi:10.1242/dev.100107
Fraser, M. J., Smith, G. E. and Summers, M. D. (1983). Acquisition of host cell DNA sequences by baculoviruses: relationship between host DNA insertions and FP mutants of Autographa californica and Galleria mellonella nuclear polyhedrosis viruses. *J. Virol.* **47**, 287-300. doi:10.1128/JVI.47.2.287-300.1983
Fraser, M. J., Clszczon, T., Elick, T. and Bauser, C. (1996). Precise excision of TTAA-specific lepidopteran transposons piggyBac (IFP2) and tagalong (TFP3) from the baculovirus genome in cell lines from two species of Lepidoptera. *Insect Mol. Biol.* **5**, 141-151. doi:10.1111/j.1365-2583.1996.tb00048.x
Funahashi, J., Okafuji, T., Ohuchi, H., Noji, S., Tanaka, H. and Nakamura, H. (1999). Role of Pax-5 in the regulation of a mid-hindbrain organizer's activity. *Dev. Growth Differ.* **41**, 59-72. doi:10.1046/j.1440-169x.1999.00401.x
Gammill, L. S., Jacques-Fricke, B. and Roffers-Agarwal, J. (2019). Embryological and genetic manipulation of chick development. *Methods Mol. Biol.* **1920**, 75-97. doi:10.1007/978-1-4939-9009-2_6
Gandhi, S., Piacentino, M. L., Vieceli, F. M. and Bronner, M. E. (2017). Optimization of CRISPR/Cas9 genome editing for loss-of-function in the early chick embryo. *Dev. Biol.* **432**, 86-97. doi:10.1016/j.ydbio.2017.08.036
Garcia-Castro, M. I., Marcelle, C. and Bronner-Fraser, M. (2002). Ectodermal Wnt function as a neural crest inducer. *Science* **13**, 13.
Garrison, B. S., Yant, S. R., Mikkelsen, J. G. and Kay, M. A. (2007). Postintegrative gene silencing within the Sleeping Beauty transposition system. *Mol. Cell. Biol.* **27**, 8824-8833. doi:10.1128/MCB.00498-07
Geurts, A. M., Yang, Y., Clark, K. J., Liu, G., Cui, Z., Dupuy, A. J., Bell, J. B., Largaespada, D. A. and Hackett, P. B. (2003). Gene transfer into genomes of human cells by the sleeping beauty transposon system. *Mol. Ther.* **8**, 108-117. doi:10.1016/S1525-0016(03)00099-6

Giovagnoli, S., Tsai, T. and DeLuca, P. P. (2010). Formulation and release behavior of doxycycline-alginate hydrogel microparticles embedded into pluronic F127 thermogels as a potential new vehicle for doxycycline intradermal sustained delivery. *AAPS PharmSciTech.* **11**, 212-220. doi:10.1208/s12249-009-9361-8

Gossen, M., Freundlieb, S., Bender, G., Muller, G., Hillen, W. and Bujard, H. (1995). Transcriptional activation by tetracyclines in mammalian cells. *Science* **268**, 1766-1769. doi:10.1126/science.7792603

Hall, J., Jheon, A. H., Ealba, E. L., Eames, B. F., Butcher, K. D., Mak, S.-S., Ladher, R., Alliston, T. and Schneider, R. A. (2014). Evolution of a developmental mechanism: Species-specific regulation of the cell cycle and the timing of events during craniofacial osteogenesis. *Dev. Biol.* **385**, 380-395. doi:10.1016/j.ydbio.2013.11.011

Hamburger, V. and Hamilton, H. L. (1951). A series of normal stages in the development of the chick embryo. *J. Morphol.* **88**, 49-92. doi:10.1002/jmor.1050880104

Hamilton, H. L. (1965). *Lillie's Development of the Chick: An Introduction to Embryology*, 3rd edn. New York: Holt, Rinehart and Winston.

Harris, M. P., Linkhart, B. L. and Fallon, J. F. (2004). Bmp7 mediates early signaling events during induction of chick epidermal organs. *Dev. Dyn.* **231**, 22-32. doi:10.1002/dvdy.20096

Heinz, N., Schambach, A., Galla, M., Maetzig, T., Baum, C., Loew, R. and Schiedlmeier, B. (2011). Retroviral and transposon-based tet-regulated all-in-one vectors with reduced background expression and improved dynamic range. *Hum. Gene. Ther.* **22**, 166-176. doi:10.1089/hum.2010.099

Heinz, N., Hennig, K. and Loew, R. (2013). Graded or threshold response of the tet-controlled gene expression: all depends on the concentration of the transactivator. *BMC Biotechnol.* **13**, 5. doi:10.1186/1472-6750-13-5

Herr, R., Wöhrle, F. U., Danke, C., Berens, C. and Brummer, T. (2011). A novel MCF-10A line allowing conditional oncogene expression in 3D culture. *Cell Commun. Signal.* **9**, 17. doi:10.1186/1478-811X-9-17

Hickman, A. B., Chandler, M. and Dyda, F. (2010). Integrating prokaryotes and eukaryotes: DNA transposases in light of structure. *Crit. Rev. Biochem. Mol. Biol.* **45**, 50-69. doi:10.3109/10409230903505596

Hollister, J. D. and Gaut, B. S. (2009). Epigenetic silencing of transposable elements: a trade-off between reduced transposition and deleterious effects on neighboring gene expression. *Genome Res.* **19**, 1419-1428. doi:10.1101/gr.091678.109

Holm, S. (1979). A Simple Sequentially Rejective Multiple Test Procedure. *Scandinavian Journal of Statistics* **6**, 65-70.

Huang, X., Guo, H., Tammana, S., Jung, Y.-C., Mellgren, E., Bassi, P., Cao, Q., Tu, Z. J., Kim, Y. C., Ekker, S. C. et al. (2010). Gene transfer efficiency and genome-wide integration profiling of Sleeping Beauty, Tol2, and piggyBac transposons in human primary T cells. *Mol. Ther.* **18**, 1803-1813. doi:10.1038/mt.2010.141

Hudecek, M., Izsvák, Z., Johnen, S., Renner, M., Thumann, G. and Ivics, Z. (2017). Going non-viral: the Sleeping Beauty transposon system breaks on through to the clinical side. *Crit. Rev. Biochem. Mol. Biol.* **52**, 355-380. doi:10.1080/10409238.2017.1304354

Hughes, S. H. (2004). The RCAS vector system. *Folia biologica* **50**, 107-119.

Huss, D., Benazeraf, B., Wallingford, A., Filla, M., Yang, J., Fraser, S. E. and Lansford, R. (2015). A transgenic quail model that enables dynamic imaging of amniote embryogenesis. *Development* **142**, 2850-2859. doi:10.1242/dev.121392

Itasaki, N., Bel-Vialar, S. and Krumlauf, R. (1999). 'Shocking' developments in chick embryology: electroporation and in ovo gene expression. *Nat. Cell Biol.* **1**, E203-E207. doi:10.1038/70231

Ivics, Z., Hackett, P. B., Plasterk, R. H. and Izsvak, Z. (1997). Molecular reconstruction of Sleeping Beauty, a Tc1-like transposon from fish, and its transposition in human cells. *Cell* **91**, 501-510. doi:10.1016/S0092-8674(00)80436-5

Janssen, A., Colmenares, S. U. and Karpen, G. H. (2018). Heterochromatin: guardian of the genome. *Annu. Rev. Cell Dev. Biol.* **34**, 265-288. doi:10.1146/annurev-cellbio-100617-062653

Jheon, A. H. and Schneider, R. A. (2009). The cells that fill the bill: neural crest and the evolution of craniofacial development. *J. Dent. Res.* **88**, 12-21. doi:10.1177/0022034508327757

Jhingory, S., Wu, C.-Y. and Taneyhill, L. A. (2010). Novel insight into the function and regulation of αN-catenin by Snail2 during chick neural crest cell migration. *Dev. Biol.* **344**, 896-910. doi:10.1016/j.ydbio.2010.06.006

Johnston, M. C. (1966). A radioautographic study of the migration and fate of cranial neural crest cells in the chick embryo. *Anat. Rec.* **156**, 143-155. doi:10.1002/ar.1091560204

Jordan, B. J., Vogel, S., Stark, M. R. and Beckstead, R. B. (2014). Expression of green fluorescent protein in the chicken using in vivo transfection of the piggyBac transposon. *J. Biotechnol.* **173**, 86-89. doi:10.1016/j.jbiotec.2014.01.016

June Byun, S., Yuk, S.-S., Jang, Y.-J., Choi, H., Jeon, M.-H., Erdene-Ochir, T. O., Kwon, J.-H., Noh, J.-Y., Sun Kim, J., Gyu Yoo, J. et al. (2017). Transgenic chickens expressing the 3D8 single chain variable fragment protein suppress avian influenza transmission. *Sci. Rep.* **7**, 5938. doi:10.1038/s41598-017-05270-8

Kardon, G., Harfe, B. D. and Tabin, C. J. (2003). A Tcf4-positive mesodermal population provides a prepattern for vertebrate limb muscle patterning. *Dev. Cell* **5**, 937-944. doi:10.1016/S1534-5807(03)00360-5

Kawakami, K. (2007). Tol2: a versatile gene transfer vector in vertebrates. *Genome Biol.* **8** Suppl. 1, S7. doi:10.1186/gb-2007-8-s1-s7

Kim, J. H., Lee, S.-R., Li, L.-H., Park, H.-J., Park, J.-H., Lee, K.-Y., Kim, M.-K., Shin, B. A. and Choi, S.-Y. (2011). High cleavage efficiency of a 2A peptide derived from porcine teschovirus-1 in human cell lines, zebrafish and mice. *PLoS ONE* **6**, e18556. doi:10.1371/journal.pone.0018556

Koga, A., Suzuki, M., Inagaki, H., Bessho, Y. and Hori, H. (1996). Transposable element in fish. *Nature* **383**, 30. doi:10.1038/383030a0

Kohrman, A. Q., Adikes, R. C., Martinez, M. A. Q., Palmisano, N. J., Smith, J. J., Medwig-Kinney, T. N., Min, M., Sallee, M. D., Ahmed, O. B., Kim, N. et al. (2020). Visualizing the metazoan proliferation-terminal differentiation decision *in vivo*. *bioRxiv*, 2019.2012.2018.881888.

Koo, B. C., Kwon, M. S., Choi, B. R., Kim, J. H., Cho, S. K., Sohn, S. H., Cho, E. J., Lee, H. T., Chang, W., Jeon, I. et al. (2006). Production of germline transgenic chickens expressing enhanced green fluorescent protein using a MoMLV-based retrovirus vector. *FASEB J.* **20**, 2251-2260. doi:10.1096/fj.06-5866com

Kos, R., Tucker, R. P., Hall, R., Duong, T. D. and Erickson, C. A. (2003). Methods for introducing morpholinos into the chicken embryo. *Dev. Dyn.* **226**, 470-477. doi:10.1002/dvdy.10254

Kozak, M. (1986). Point mutations define a sequence flanking the AUG initiator codon that modulates translation by eukaryotic ribosomes. *Cell* **44**, 283-292. doi:10.1016/0092-8674(86)90762-2

Krull, C. E. (2004). A primer on using in ovo electroporation to analyze gene function. *Dev. Dyn.* **229**, 433-439. doi:10.1002/dvdy.10473

Kulesa, P. M. and Fraser, S. E. (2000). In ovo time-lapse analysis of chick hindbrain neural crest cell migration shows cell interactions during migration to the branchial arches. *Development* **127**, 1161-1172.

Kumamoto, T., Maurinot, F., Barry-Martinet, R., Vaslin, C., Vandormael-Pournin, S., Le, M., Lerat, M., Niculescu, D., Cohen-Tannoudji, M., Rebsam, A. et al. (2020). Direct Readout of Neural Stem Cell Transgenesis with an Integration-Coupled Gene Expression Switch. *Neuron* **107**, 617-630 e616.

Lacoste, A., Berenshteyn, F. and Brivanlou, A. H. (2009). An efficient and reversible transposable system for gene delivery and lineage-specific differentiation in human embryonic stem cells. *Cell Stem Cell* **5**, 332-342. doi:10.1016/j.stem.2009.07.011

Larsen, C. W., Zeltser, L. M. and Lumsden, A. (2001). Boundary formation and compartition in the avian diencephalon. *J. Neurosci.* **21**, 4699-4711. doi:10.1523/JNEUROSCI.21-13-04699.2001

Le Douarin, N. and McLaren, A. (1984). *Chimeras in Developmental Biology*. London; Orlando: Academic Press.

Le Douarin, N. M. and Dieterlen-Lièvre, F. (2013). How studies on the avian embryo have opened new avenues in the understanding of development: a view about the neural and hematopoietic systems. *Dev. Growth Differ.* **55**, 1-14. doi:10.1111/dgd.12015

Le Douarin, N. M., Dieterlen-Lievre, F. and Teillet, M. (1996). Quail-chick transplantations. In *Methods in Avian Embryology* (ed. M. Bronner-Fraser), pp. 23-59. San Diego: Academic Press.

Leary, S., Underwood, W., Anthony, R., Cartner, S., Corey, D., Grandin, T., Greenacre, C., Gwaltney-Brant, S., McCrackin, M. A., Meye, R. et al. (2013). *AVMA Guidelines for the Euthanasia of Animals*. 2013 edn. Schaumburg, IL: American Veterinary Medical Association.

Lesueur, L. L., Mir, L. M. and André, F. M. (2016). Overcoming the specific toxicity of large plasmids electrotransfer in primary cells in vitro. *Mol. Ther. Nucleic Acids* **5**, e291. doi:10.1038/mtna.2016.4

Li, M. A., Turner, D. J., Ning, Z., Yusa, K., Liang, Q., Eckert, S., Rad, L., Fitzgerald, T. W., Craig, N. L. and Bradley, A. (2011). Mobilization of giant piggyBac transposons in the mouse genome. *Nucleic Acids Res.* **39**, e148. doi:10.1093/nar/gkr764

Liu, H. and Naismith, J. H. (2008). An efficient one-step site-directed deletion, insertion, single and multiple-site plasmid mutagenesis protocol. *BMC Biotechnol.* **8**, 91. doi:10.1186/1472-6750-8-91

Liu, X., Li, N., Hu, X., Zhang, R., Li, Q., Cao, D., Liu, T., Zhang, Y. and Liu, X. (2013). Efficient production of transgenic chickens based on piggyBac. *Transgenic Res.* **22**, 417-423. doi:10.1007/s11248-012-9642-y

Loew, R., Heinz, N., Hampf, M., Bujard, H. and Gossen, M. (2010). Improved Tet-responsive promoters with minimized background expression. *BMC Biotechnol.* **10**, 81. doi:10.1186/1472-6750-10-81

Logan, M. and Tabin, C. (1998). Targeted gene misexpression in chick limb buds using avian replication-competent retroviruses. *Methods* **14**, 407-420. doi:10.1006/meth.1998.0595

Lu, Y., Lin, C. and Wang, X. (2009). PiggyBac transgenic strategies in the developing chicken spinal cord. *Nucleic Acids Res.* **37**, e141. doi:10.1093/nar/gkp686

Lwigale, P. Y. and Schneider, R. A. (2008). Other chimeras: quail-duck and mouse-chick. *Methods Cell Biol.* **87**, 59-74. doi:10.1016/S0091-679X(08)00203-3

Lwigale, P. Y., Conrad, G. W. and Bronner-Fraser, M. (2004). Graded potential of neural crest to form cornea, sensory neurons and cartilage along the rostrocaudal axis. *Development* **131**, 1979-1991. doi:10.1242/dev.01106

Lwigale, P. Y., Cressy, P. A. and Bronner-Fraser, M. (2005). Corneal keratocytes retain neural crest progenitor cell properties. *Dev. Biol.* **288**, 284-293. doi:10.1016/j.ydbio.2005.09.046
Macdonald, J., Taylor, L., Sherman, A., Kawakami, K., Takahashi, Y., Sang, H. M. and McGrew, M. J. (2012). Efficient genetic modification and germ-line transmission of primordial germ cells using piggyBac and Tol2 transposons. *Proc. Natl. Acad. Sci. USA* **109**, E1466-E1472. doi:10.1073/pnas.1118715109
Mandegar, M. A., Huebsch, N., Frolov, E. B., Shin, E., Truong, A., Olvera, M. P., Chan, A. H., Miyaoka, Y., Holmes, K., Spencer, C. I. et al. (2016). CRISPR interference efficiently induces specific and reversible gene silencing in human iPSCs. *Cell Stem Cell* **18**, 541-553. doi:10.1016/j.stem.2016.01.022
Martik, M. L. and Bronner, M. E. (2017). Regulatory logic underlying diversification of the neural crest. *Trends Genet.* **33**, 715-727. doi:10.1016/j.tig.2017.07.015
McGrew, M. J., Sherman, A., Ellard, F. M., Lillico, S. G., Gilhooley, H. J., Kingsman, A. J., Mitrophanous, K. A. and Sang, H. (2004). Efficient production of germline transgenic chickens using lentiviral vectors. *EMBO Rep.* **5**, 728-733. doi:10.1038/sj.embor.7400171
McLarren, K. W., Litsiou, A. and Streit, A. (2003). DLX5 positions the neural crest and preplacode region at the border of the neural plate. *Dev. Biol.* **259**, 34-47. doi:10.1016/S0012-1606(03)00177-5
McLennan, R. and Kulesa, P. M. (2007). In vivo analysis reveals a critical role for neuropilin-1 in cranial neural crest cell migration in chick. *Dev. Biol.* **301**, 227-239. doi:10.1016/j.ydbio.2006.08.019
McLennan, R. and Kulesa, P. M. (2019). In ovo electroporation of plasmid DNA and morpholinos into specific tissues during early embryogenesis. *Methods Mol. Biol.* **1976**, 71-82. doi:10.1007/978-1-4939-9412-0_6
Megason, S. G. and McMahon, A. P. (2002). A mitogen gradient of dorsal midline Wnts organizes growth in the CNS. *Development* **129**, 2087-2098.
Meir, Y. J. and Wu, S. C. (2011). Transposon-based vector systems for gene therapy clinical trials: challenges and considerations. *Chang Gung Med. J.* **34**, 565-579.
Meir, Y.-J. J., Weirauch, M. T., Yang, H.-S., Chung, P.-C., Yu, R. K. and Wu, S. C.-Y. (2011). Genome-wide target profiling of piggyBac and Tol2 in HEK 293: pros and cons for gene discovery and gene therapy. *BMC Biotechnol.* **11**, 28. doi:10.1186/1472-6750-11-28
Merrill, A. E., Eames, B. F., Weston, S. J., Heath, T. and Schneider, R. A. (2008). Mesenchyme-dependent BMP signaling directs the timing of mandibular osteogenesis. *Development* **135**, 1223-1234. doi:10.1242/dev.015933
Miller, A. M., Munkonge, F. M., Alton, E. W. F. W. and Dean, D. A. (2009). Identification of protein cofactors necessary for sequence-specific plasmid DNA nuclear import. *Mol. Ther.* **17**, 1897-1903. doi:10.1038/mt.2009.127
Momose, T., Tonegawa, A., Takeuchi, J., Ogawa, H., Umesono, K. and Yasuda, K. (1999). Efficient targeting of gene expression in chick embryos by microelectroporation. *Dev. Growth Differ.* **41**, 335-344. doi:10.1046/j.1440-169X.1999.413437.x
Morgan, B. A. and Fekete, D. M. (1996). Manipulating gene expression with replication-competent retroviruses. In *Methods in Avian Embryology* (ed. M. Bronner-Fraser), pp. 186-217. San Diego: Academic Press.
Morin, V., Véron, N. and Marcelle, C. (2017). CRISPR/Cas9 in the chicken embryo. In *Avian and Reptilian Developmental Biology: Methods and Protocols* (ed. G. Sheng), p. 1 online resource (xii, 365 pages). New York: Humana Press: Springer.
Nakamura, H. and Funahashi, J.-I. (2001). Introduction of DNA into chick embryos by in ovo electroporation. *Methods* **24**, 43-48. doi:10.1006/meth.2001.1155
Nakamura, H., Katahira, T., Sato, T., Watanabe, Y. and Funahashi, J.-I. (2004). Gain- and loss-of-function in chick embryos by electroporation. *Mech. Dev.* **121**, 1137-1143. doi:10.1016/j.mod.2004.05.013
Noden, D. M. (1975). An analysis of the migratory behavior of avian cephalic neural crest cells. *Dev. Biol.* **42**, 106-130. doi:10.1016/0012-1606(75)90318-8
Noden, D. M. (1984). The use of chimeras in analyses of craniofacial development. In *Chimeras in Developmental Biology* (ed. N. Le Douarin and A. McLaren), pp. 241-280. London; Orlando: Academic Press.
Noden, D. M. and Schneider, R. A. (2006). Neural crest cells and the community of plan for craniofacial development: historical debates and current perspectives. *Adv. Exp. Med. Biol.* **589**, 1-23. doi:10.1007/978-0-387-46954-6_1
Norrman, K., Fischer, Y., Bonnamy, B., Wolfhagen Sand, F., Ravassard, P. and Semb, H. (2010). Quantitative comparison of constitutive promoters in human ES cells. *PLoS ONE* **5**, e12413. doi:10.1371/journal.pone.0012413
Núñez-León, D., Aguirre-Fernández, G., Steiner, A., Nagashima, H., Jensen, P., Stoeckli, E., Schneider, R. A. and Sánchez-Villagra, M. R. (2019). Morphological diversity of integumentary traits in fowl domestication: insights from disparity analysis and embryonic development. *Dev. Dyn.* **248**, 1044-1058. doi:10.1002/dvdy.105
Ottaviani, A., Rival-Gervier, S., Boussouar, A., Foerster, A. M., Rondier, D., Sacconi, S., Desnuelle, C., Gilson, E. and Magdinier, F. (2009). The D4Z4 macrosatellite repeat acts as a CTCF and A-type lamins-dependent insulator in facio-scapulo-humeral dystrophy. *PLoS Genet.* **5**, e1000394. doi:10.1371/journal.pgen.1000394
Pannell, D. and Ellis, J. (2001). Silencing of gene expression: implications for design of retrovirus vectors. *Rev. Med. Virol.* **11**, 205-217. doi:10.1002/rmv.316
Park, S. H., Kim, J. N., Park, T. S., Lee, S. D., Kim, T. H., Han, B. K. and Han, J. Y. (2010). CpG methylation modulates tissue-specific expression of a transgene in chickens. *Theriogenology* **74**, 805-816.e801. doi:10.1016/j.theriogenology.2010.04.005
Pourquié, O. (2018). Somite formation in the chicken embryo. *Int. J. Dev. Biol.* **62**, 57-62. doi:10.1387/ijdb.180036op
Qi, L. S., Larson, M. H., Gilbert, L. A., Doudna, J. A., Weissman, J. S., Arkin, A. P. and Lim, W. A. (2013). Repurposing CRISPR as an RNA-guided platform for sequence-specific control of gene expression. *Cell* **152**, 1173-1183. doi:10.1016/j.cell.2013.02.022
Qin, J. Y., Zhang, L., Clift, K. L., Hulur, I., Xiang, A. P., Ren, B.-Z. and Lahn, B. T. (2010). Systematic comparison of constitutive promoters and the doxycycline-inducible promoter. *PLoS ONE* **5**, e10611. doi:10.1371/journal.pone.0010611
Rao, M., Baraban, J. H., Rajaii, F. and Sockanathan, S. (2004). In vivo comparative study of RNAi methodologies by in ovo electroporation in the chick embryo. *Dev. Dyn.* **231**, 592-600. doi:10.1002/dvdy.20161
Reberšek, M. (2017). Beyond electroporation pulse parameters: from application to evaluation. In *Handbook of Electroporation* (ed. D. Miklavcic), pp. 1-21. Cham: Springer International Publishing.
Ricklefs, R. E. and Starck, J. M. (1998). Embryonic growth and development. In *Avian Growth and Development: Evolution within the Altricial-Precocial Spectrum* (ed. J. M. Starck and R. E. Ricklefs), pp. 31-58. New York: Oxford University Press.
Roney, I. J., Rudner, A. D., Couture, J.-F. and Kærn, M. (2016). Improvement of the reverse tetracycline transactivator by single amino acid substitutions that reduce leaky target gene expression to undetectable levels. *Sci. Rep.* **6**, 27697. doi:10.1038/srep27697
Rostovskaya, M., Naumann, R., Fu, J., Obst, M., Mueller, D., Stewart, A. F. and Anastassiadis, K. (2013). Transposon mediated BAC transgenesis via pronuclear injection of mouse zygotes. *Genesis* **51**, 135-141. doi:10.1002/dvg.22362
Sang, H. (2006). Transgenesis sunny-side up. *Nat. Biotechnol.* **24**, 955-956. doi:10.1038/nbt0806-955
Sato, Y., Kasai, T., Nakagawa, S., Tanabe, K., Watanabe, T., Kawakami, K. and Takahashi, Y. (2007). Stable integration and conditional expression of electroporated transgenes in chicken embryos. *Dev. Biol.* **305**, 616-624. doi:10.1016/j.ydbio.2007.01.043
Sato, Y., Poynter, G., Huss, D., Filla, M. B., Czirok, A., Rongish, B. J., Little, C. D., Fraser, S. E. and Lansford, R. (2010). Dynamic analysis of vascular morphogenesis using transgenic quail embryos. *PLoS ONE* **5**, e12674. doi:10.1371/journal.pone.0012674
Sauka-Spengler, T. and Barembaum, M. (2008). Gain- and loss-of-function approaches in the chick embryo. *Methods Cell Biol.* **87**, 237-256. doi:10.1016/S0091-679X(08)00212-4
Sauka-Spengler, T. and Bronner-Fraser, M. (2008). A gene regulatory network orchestrates neural crest formation. *Nat. Rev. Mol. Cell Biol.* **9**, 557-568. doi:10.1038/nrm2428
Scaal, M., Gros, J., Lesbros, C. and Marcelle, C. (2004). In ovo electroporation of avian somites. *Dev. Dyn.* **229**, 643-650. doi:10.1002/dvdy.10433
Schneider, R. A. (1999). Neural crest can form cartilages normally derived from mesoderm during development of the avian head skeleton. *Dev. Biol.* **208**, 441-455. doi:10.1006/dbio.1999.9213
Schneider, R. A. (2007). How to tweak a beak: molecular techniques for studying the evolution of size and shape in Darwin's finches and other birds. *BioEssays* **29**, 1-6. doi:10.1002/bies.20517
Schneider, R. A. (2018). Neural crest and the origin of species-specific pattern. *Genesis* **56**, e23219. doi:10.1002/dvg.23219
Schneider, R. A., Hu, D., Rubenstein, J. L., Maden, M. and Helms, J. A. (2001). Local retinoid signaling coordinates forebrain and facial morphogenesis by maintaining FGF8 and SHH. *Development* **128**, 2755-2767.
Serbedzija, G. N., Bronner-Fraser, M. and Fraser, S. E. (1989). A vital dye analysis of the timing and pathways of avian trunk neural crest cell migration. *Development* **106**, 809-816.
Serralbo, O., Picard, C. A. and Marcelle, C. (2013). Long-term, inducible gene loss-of-function in the chicken embryo. *Genesis* **51**, 372-380. doi:10.1002/dvg.22388
Shaner, N. C., Lambert, G. G., Chammas, A., Ni, Y., Cranfill, P. J., Baird, M. A., Sell, B. R., Allen, J. R., Day, R. N., Israelsson, M. et al. (2013). A bright monomeric green fluorescent protein derived from Branchiostoma lanceolatum. *Nat. Methods* **10**, 407-409. doi:10.1038/nmeth.2413
Simkin, J. E., Zhang, D., Ighaniyan, S. and Newgreen, D. F. (2014). Parameters affecting efficiency of in ovo electroporation of the avian neural tube and crest. *Dev. Dyn.* **243**, 1440-1447. doi:10.1002/dvdy.24163
Smith, S. S., Dole, N. S., Franceschetti, T., Hrdlicka, H. C. and Delany, A. M. (2016). MicroRNA-433 dampens glucocorticoid receptor signaling, impacting circadian rhythm and osteoblastic gene expression. *J. Biol. Chem.* **291**, 21717-21728. doi:10.1074/jbc.M116.737890
Spencer, S. L., Cappell, S. D., Tsai, F.-C., Overton, K. W., Wang, C. L. and Meyer, T. (2013). The proliferation-quiescence decision is controlled by a bifurcation in CDK2 activity at mitotic exit. *Cell* **155**, 369-383. doi:10.1016/j.cell.2013.08.062

Starck, J. M. and Ricklefs, R. E. (1998). *Avian Growth and Development: Evolution within the Altricial-Precocial Spectrum*. New York: Oxford University Press.
Stern, C. D. (2005). The chick: a great model system becomes even greater. *Dev. Cell* **8**, 9-17. doi:10.1016/S1534-5807(04)00425-3
Stocker, K. M., Brown, A. M. C. and Ciment, G. (1993). Gene transfer of LacZ into avian neural tube and neural crest by retroviral infection of grafted embryonic tissues. *J. Neurosci. Res.* **34**, 135-145. doi:10.1002/jnr.490340114
Swartz, M., Eberhart, J., Mastick, G. S. and Krull, C. E. (2001). Sparking new frontiers: using in vivo electroporation for genetic manipulations. *Dev. Biol.* **233**, 13-21. doi:10.1006/dbio.2001.0181
Szymczak, A. L., Workman, C. J., Wang, Y., Vignali, K. M., Dilioglou, S., Vanin, E. F. and Vignali, D. A. (2004). Correction of multi-gene deficiency in vivo using a single 'self-cleaving' 2A peptide-based retroviral vector. *Nat. Biotechnol.* **22**, 589-594. doi:10.1038/nbt957
Takahashi, Y., Watanabe, T., Nakagawa, S., Kawakami, K. and Sato, Y. (2008). Transposon-mediated stable integration and tetracycline-inducible expression of electroporated transgenes in chicken embryos. *Methods Cell Biol.* **87**, 271-280. doi:10.1016/S0091-679X(08)00214-8
Tokita, M. and Schneider, R. A. (2009). Developmental origins of species-specific muscle pattern. *Dev. Biol.* **331**, 311-325. doi:10.1016/j.ydbio.2009.05.548
Trainor, P. A., Ariza-McNaughton, L. and Krumlauf, R. (2002). Role of the isthmus and FGFs in resolving the paradox of neural crest plasticity and prepatterning. *Science* **295**, 1288-1291. doi:10.1126/science.1064540
Tsujino, K., Okuzaki, Y., Hibino, N., Kawamura, K., Saito, S., Ozaki, Y., Ishishita, S., Kuroiwa, A., Iijima, S., Matsuda, Y. et al. (2019). Identification of transgene integration site and anatomical properties of fluorescence intensity in a EGFP transgenic chicken line. *Dev. Growth Differ.* **61**, 393-401. doi:10.1111/dgd.12631
Tucker, R. P. (2001). Abnormal neural crest cell migration after the in vivo knockdown of tenascin-C expression with morpholino antisense oligonucleotides. *Dev. Dyn.* **222**, 115-119. doi:10.1002/dvdy.1171
Utvik, J. K., Nja, A. and Gundersen, K. (1999). DNA injection into single cells of intact mice. *Hum. Gene. Ther.* **10**, 291-300. doi:10.1089/10430349950019075
van de Lavoir, M.-C., Diamond, J. H., Leighton, P. A., Mather-Love, C., Heyer, B. S., Bradshaw, R., Kerchner, A., Hooi, L. T., Gessaro, T. M., Swanberg, S. E. et al. (2006a). Germline transmission of genetically modified primordial germ cells. *Nature* **441**, 766-769. doi:10.1038/nature04831
van de Lavoir, M.-C., Mather-Love, C., Leighton, P., Diamond, J. H., Heyer, B. S., Roberts, R., Zhu, L., Winters-Digiacinto, P., Kerchner, A., Gessaro, T. et al. (2006b). High-grade transgenic somatic chimeras from chicken embryonic stem cells. *Mech. Dev.* **123**, 31-41. doi:10.1016/j.mod.2005.10.002
Vandenbroucke, R. E., Lucas, B., Demeester, J., De Smedt, S. C. and Sanders, N. N. (2007). Nuclear accumulation of plasmid DNA can be enhanced by non-selective gating of the nuclear pore. *Nucleic Acids Res.* **35**, e86. doi:10.1093/nar/gkm440
Wang, H., Bonnet, A., Delfini, M. C., Kawakami, K., Takahashi, Y. and Duprez, D. (2011). Stable, conditional, and muscle-fiber-specific expression of electroporated transgenes in chick limb muscle cells. *Dev. Dyn.* **240**, 1223-1232. doi:10.1002/dvdy.22498
Watanabe, T., Saito, D., Tanabe, K., Suetsugu, R., Nakaya, Y., Nakagawa, S. and Takahashi, Y. (2007). Tet-on inducible system combined with in ovo electroporation dissects multiple roles of genes in somitogenesis of chicken embryos. *Dev. Biol.* **305**, 625-636. doi:10.1016/j.ydbio.2007.01.042
Wen, S., Zhang, H., Li, Y., Wang, N., Zhang, W., Yang, K., Wu, N., Chen, X., Deng, F., Liao, Z. et al. (2014). Characterization of constitutive promoters for piggyBac transposon-mediated stable transgene expression in mesenchymal stem cells (MSCs). *PLoS ONE* **9**, e94397. doi:10.1371/journal.pone.0094397
Williams, R. M., Senanayake, U., Artibani, M., Taylor, G., Wells, D., Ahmed, A. A. and Sauka-Spengler, T. (2018). Genome and epigenome engineering CRISPR toolkit for in vivo modulation of cis-regulatory interactions and gene expression in the chicken embryo. *Development* **145**, dev160333. doi:10.1242/dev.160333
Woronowicz, K. C., Gline, S. E., Herfat, S. T., Fields, A. J. and Schneider, R. A. (2018). FGF and TGFbeta signaling link form and function during jaw development and evolution. *Dev. Biol.* **444** Suppl. 1, S219-S236. doi:10.1016/j.ydbio.2018.05.002
Wu, C. Y. and Taneyhill, L. A. (2019). Cadherin-7 mediates proper neural crest cell-placodal neuron interactions during trigeminal ganglion assembly. *Genesis* **57**, e23264. doi:10.1002/dvg.23264
Wu, S. C.-Y., Meir, Y.-J. J., Coates, C. J., Handler, A. M., Pelczar, P., Moisyadi, S. and Kaminski, J. M. (2006). piggyBac is a flexible and highly active transposon as compared to sleeping beauty, Tol2, and Mos1 in mammalian cells. *Proc. Natl. Acad. Sci. USA* **103**, 15008-15013. doi:10.1073/pnas.0606979103
Xia, X., Zhang, Y., Zieth, C. R. and Zhang, S.-C. (2007). Transgenes delivered by lentiviral vector are suppressed in human embryonic stem cells in a promoter-dependent manner. *Stem Cells Dev.* **16**, 167-176. doi:10.1089/scd.2006.0057
Yang, C. Q., Li, X. Y., Li, Q., Fu, S. L., Li, H., Guo, Z. K., Lin, J. T. and Zhao, S. T. (2014). Evaluation of three different promoters driving gene expression in developing chicken embryo by using in vivo electroporation. *Genet. Mol. Res.* **13**, 1270-1277. doi:10.4238/2014.February.27.12
Yeo, N. C., Chavez, A., Lance-Byrne, A., Chan, Y., Menn, D., Milanova, D., Kuo, C.-C., Guo, X., Sharma, S., Tung, A. et al. (2018). An enhanced CRISPR repressor for targeted mammalian gene regulation. *Nat. Methods* **15**, 611-616. doi:10.1038/s41592-018-0048-5
Yin, W., Xiang, P. and Li, Q. (2005). Investigations of the effect of DNA size in transient transfection assay using dual luciferase system. *Anal. Biochem.* **346**, 289-294. doi:10.1016/j.ab.2005.08.029
Yokota, Y., Saito, D., Tadokoro, R. and Takahashi, Y. (2011). Genomically integrated transgenes are stably and conditionally expressed in neural crest cell-specific lineages. *Dev. Biol.* **353**, 382-395. doi:10.1016/j.ydbio.2011.02.001
Young, J. L., Benoit, J. N. and Dean, D. A. (2003). Effect of a DNA nuclear targeting sequence on gene transfer and expression of plasmids in the intact vasculature. *Gene Ther.* **10**, 1465-1470. doi:10.1038/sj.gt.3302021
Yuan, Y.-W. and Wessler, S. R. (2011). The catalytic domain of all eukaryotic cut-and-paste transposase superfamilies. *Proc. Natl. Acad. Sci. USA* **108**, 7884-7889. doi:10.1073/pnas.1104208108
Yusa, K. (2015). piggyBac Transposon. *Microbiol. Spectr.* **3**, MDNA3-0028-2014. doi:10.1128/microbiolspec.MDNA3-0028-2014
Yusa, K., Zhou, L., Li, M. A., Bradley, A. and Craig, N. L. (2011). A hyperactive piggyBac transposase for mammalian applications. *Proc. Natl. Acad. Sci. USA* **108**, 1531-1536. doi:10.1073/pnas.1008322108
Zhou, X., Vink, M., Klaver, B., Berkhout, B. and Das, A. T. (2006). Optimization of the Tet-On system for regulated gene expression through viral evolution. *Gene Ther.* **13**, 1382-1390. doi:10.1038/sj.gt.3302780

Table S1

qPCR primers	
CXCL14 F3 Chick	5'-GCAGAAGGAGTAAAGTGCAA-3'
CXCL14 R3 Chick	5'-GTACCACTTGAGCAGCCTCA-3'
Runx2 F1 CQ DC	5'-CCGTCCTACTTGAGCCAGAT-3'
Runx2 R1 CQ DC	5'-ACGTCGGTGATGGCTGGAAG-3'
MMP13_F1_universal_SS	5'-CCTGATGATGATGTGCAAG-3'
MMP13_R1_universal_SS	5'-CCTGTCCTTGAAGACCAG-3'
Gas1_F1_Chick_Quail_ZV	5'-CCGCTACATGGCCTACTG-3'
Gas1_R2_Chick_ZV	5'-CTTGACCGACTCGCAGAT-3'

Cloning primers	
GAS1 FL F1 CQ DC	5'-TGGATTGATGCGAGGAGACC-3'
GAS1 FL R1 CQ DC	5'-CACACGGGGACAGACACAC-3'
pTet GAS1 F1 CQ DC	5'-ACCCTCGTAAAGCCGCCACCATGCCGGCCCGCCCG-3'
pTet GAS1 R1 CQ DC	5'-GCCGCTTCACTTGTACTGCACTAGAGCGGCGGTAGCAGC-3'
CXCL14 5UTR C F1 DC	5'-GAACACAAGACAGAACCCCG-3'
CXCL14 3UTR U R1 DC	5'-GGTGTGAAATCTGAAGTGCA-3'
pTet Cxcl14 F1 U DC	5'-ACCCTCGTAAAGCCGCCACCATGAAGCTCCTGACAGC-3'
pTet Cxcl14 R1 CQ DC	5'-GCCGCTTCACTTGTACTGCACGCCGCCTCCTATTCTTCAT-3'
Mmp13 C F1 FL DC	5'-ATGCAACCCAGACTTTCAGC-3'
Mmp13 C R1 FL DC	5'-GGTAGTCAGTGCTTGTTCGC-3'
pTet MMP13 F1 C DC	5'-ACCCTCGTAAAGCCGCCACCATGCAACCCAGACTTTCAGC-3'
pTet MMP13 R1 CQ DC	5'-GCCGCTTCACTTGTACTGCATCAGCACCAAAATAAGGAGT-3'
Runx2 C F2 FL DC	5'-ATGGCATCAAACAGCCTCTT-3'
Runx2 U R1 FL DC	5'-TCAGTACGGCCTCCAAACG-3'
pTET Runx2 F1 CQ DC	5'-ACCCTCGTAAAGCCGCCACCATGGCATCAAACAGCCTCTT-3'
pTET Runx2 R1 U DC	5'-GCCGCTTCACTTGTACTGCATCAGTACGGCCTCCAAACG-3'
pTet H2B F1 DC	5'-GGCCTTTCGGCCGCCACCATGCCAGAGCCAGCGAAG-3'
pTet H2B R1 DC	5'-CCTCCTCGCCCTTGCTCACCATGGTGGCGACCGGTGGAAC-3'
pNanoPB mPGK R2 DC	5'-GGTGGCGGCCGAAAGGCCCGGAGATGAGG-3'
pPID2 Tet Bi F1 DC	5'-GGAGCGACAGTGGTAGACAGCCCCATAGAGCCC-3'
Fluor Tet Bi F1 DC	5'-ATGGTGAGCAAGGGCGAGG-3'
rbGlob Tet Bi R1 DC	5'-TTAAGAGTCGTCACCTGCAGTACAAGTGAAGCGGCCGGCC-3'
Tet rbGlob F1 DC	5'-CTGCAGGTGACGACTCTTAAGGTGGCGGCTTTACGAGGGTAGGAAGTGG-3'
Ori F1 DC	5'-GCCTCACTGATTAAGCATTGGTACCCGTAGAAAAGATCAAAGGATC-3'
Ori R1 DC	5'-ACATATTTCTCGAGATATCGAATTCGTTTTTCCATAGGCTCCGCC-3'
BlaR F1 DC	5'-GGAAAAACGAATTCGATATCTCGAGAAATATGTATCCGCTCATGAGAC-3'
BlaR R1 DC	5'-GATCCTTTGATCTTTTCTACGGGTACCAATGCTTAATCAGTGAGGC-3'
pNano PB 5'LTR R DC	5'-GGCTGTCCCTGATATCTATAACA-3'

pNanoPB mPGK F1 DC	5’-TATAGATATCAGGGACAGCCGGGTAGGGGAGGCGCTTT-3’
pNanoPB mPGK R2 DC	5’-GGTGGCGGCCGAAAGGCCCGGAGATGAGG-3’
pNano rbGlob R1 DC	5’-TCATGAGCGGATACATATTTGAGAAGAGGGACAGCTATGA-3’
pNano PB 3'LTR F2 DC	5’-GGCTGTCCCTCATAAAAGTTTTGTTACTTTATAGA-3’
pNanoPB rbGlob R1 DC	5’-AACTTTTATGAGGGACAGCCGAGAAGAGGGACAGCTATGA-3’
pNano PB 3'LTR R2 DC	5’-GAGCGGATACATATTTCTCGTTAACCCTAGAAAGATAATC-3’
Fluor F1 DC	5’-ATGGTGAGCAAGGGCGAGG-3’
pNano PB 3'LTR R2 DC	5’-GAGCGGATACATATTTCTCGTTAACCCTAGAAAGATAATC-3’
pNano HyPBase F2 DC	5’-CCTCATCTCCGGGCCTTTCGAATTCGCCGCCACCATGGG-3’
pNano HyPBase R2 DC	5’-CCGGCCGCTTCACTTGTATCAGAAACAGCTCTGGCACA-3’
pNano mPGK F1 DC	5’-GGCGGAGCCTATGGAAAAACGGGTAGGGGAGGCGCTTT-3’
pPID PGK F1 DC	5’-GGAGGGAGCGACAGTGGTGGGTAGGGGAGGCGCTT-3’
pNanoPB rbGlob F1 DC	5’-TACAAGTGAAGCGGCCGG-3’
pE Kozak F1 DC	5’-GCCTTTCGATTGCCGCCACC-3’
pNanoPB IRES F1	5’-CCTCATCTCCGGGCCTTTCGGAATTCGTGGACTCTCGAGG-3’
Tet mNG R1 DC	5’-GCAACTAGAAGGCACAGTCGTTACCCGGGGAGCATGTCAA-3’
Tet mNG F1 DC	5’-TGGAGGAGAACCCCGGCCCCATGTCTAGACTGGACAAGAGC-3’
mNG P2A R1 DC	5’-GGGGCCGGGGTTCTCCTCCA-3’
Tet Bi mNG F1 DC	5’-CCTCATCTCCGGGCCTTTCGGCCGCCACCATGGTGAGCAAGGGCGA-3’
Tet Bi FL F1 DC	5’-GAAAAGCGCCTCCCCTACCCGAGAAGAGGGACAGCTATGA-3’
PGK FL F1 DC	5’-GGGTAGGGGAGGCGCTTTTC-3’
rbGlob Tet Bi R1 DC	5’-TTAAGAGTCGTCACCTGCAGTACAAGTGAAGCGGCCGGCC-3’
Tet rbGlob F1 DC	5’-CTGCAGGTGACGACTCTTAAGGTGGCGGCTTTACGAGGGTAGGAAGTGG-3’
Tet Fluor R2 DC	5’-TCCTCGCCCTTGCTCACCATGGTGGCGGCGGTGAATTCTCCAGGCGATC-3’
BGH Tet Bi F1 DC	5’-CGACTGTGCCTTCTAGTTGC-3’
Fluor Tet Bi R1 DC	5’-GCAACTAGAAGGCACAGTCGTCACTTGTACAGCTCGTCCA-3’
pPID2 Tet Bi R1 DC	5’-GAGAGCACGAGTCATCTAGAGGACAGCCATAGAGCCCA-3’

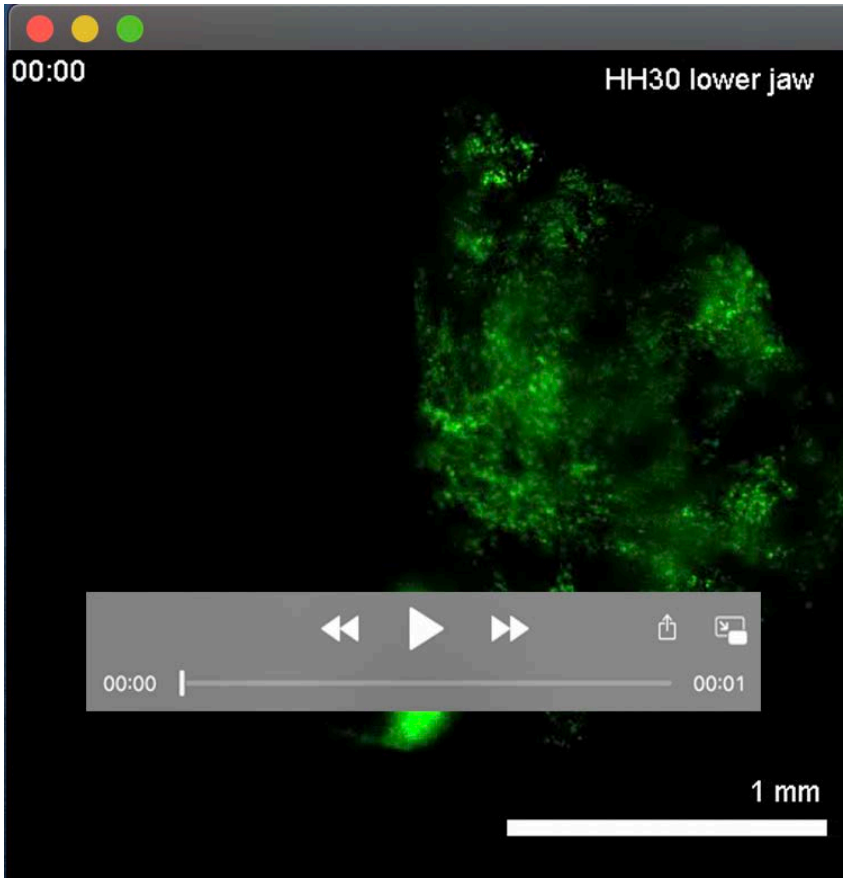

Movie 1